

Novel 2,7-Dialkyl-Substituted 5(S)-Amino-4(S)-hydroxy-8-phenyl-octanecarboxamide Transition State Peptidomimetics Are Potent and Orally Active Inhibitors of Human Renin

Richard Göschke, Stefan Stutz,[†] Vittorio Rasetti, Nissim-Claude Cohen,[‡] Joseph Rahuel, Pascal Rigollier, Hans-Peter Baum, Peter Forgiarini, Christian R. Schnell, Trixie Wagner,[§] Markus G. Gruetter,^{||} Walter Fuhrer, Walter Schilling,[⊥] Frédéric Cumin, Jeanette M. Wood, and Jürgen Maibaum*

Novartis Institutes for BioMedical Research, NOVARTIS Pharma AG, CH-4002 Basel, Switzerland

Received March 19, 2007

The action of renin is the rate-limiting step of the renin-angiotensin system (RAS), a key regulator of blood pressure. Effective renin inhibitors directly block the RAS entirely at source and, thus, may provide a vital weapon for hypertension therapy. Our efforts toward identifying novel small-molecule peptidomimetic renin inhibitors have resulted in the design of transition-state isosteres such as **1** bearing an all-carbon 8-phenyl-octanecarboxamide framework. Optimization of the extended P3 portion of **1** and extensive P2' modifications provided analogues with improved in vitro potencies in the presence of plasma. X-ray resolution of rh-renin/**38a** in the course of SAR work surprisingly unveiled the exploitation of a previously unexplored pocket (S3^{SP}) important for strong binding affinities. Several inhibitors demonstrated oral efficacy in sodium-depleted marmosets. The most potent, **38a**, induced dose-dependently a pronounced reduction in mean arterial blood pressure, paralleled by complete blockade of active plasma renin, up to 8 h post-dose. Oral bioavailability of **38a** was 16% in marmosets.

Introduction

Hypertension is currently estimated to cause 4.5% of the total global disease burden¹ and is seen as one of the most modifiable risk factors for cardiac disease. An already highly prevalent risk factor for cardiovascular disease (CVD²) throughout the industrialized world, hypertension is becoming an increasingly common health problem worldwide, estimated to cause 7.1 million premature deaths annually.¹ Despite the large number of people who suffer from hypertension worldwide, many (30%) are not aware they are hypertensive, 25% are taking medication, but their blood pressure (BP) is not controlled, 34% are taking medication and their BP is controlled, and 11% are aware but are not taking medication.² Consequently, well-tolerated effective treatments to control hypertension and associated CVDs are required.

The renin-angiotensin system (RAS) has long been established as being a key regulator of BP and body fluid volume. The RAS in normotensive humans is stimulated by a number of signals including decreased sodium plasma concentration, body fluid volume depletion, or a reduction in BP. Upon stimulation, renin, a 340 amino acid residue protein formed from pre-

prorenin,³ is released from the kidney where it is synthesized in the juxtaglomerular apparatus.⁴ In common with all aspartyl proteases, the superfamily to which it belongs, renin's active site is a long, deep cleft that can accommodate seven amino acid residues of the substrate angiotensinogen. Renin controls the first and rate-limiting step of the RAS and catalyzes the specific hydrolysis of the Leu₁₀-Val₁₁ peptide bond of the amino-terminal portion of angiotensinogen to release the decapeptide angiotensin I (Ang I). Angiotensin converting enzyme (ACE), a monomeric zinc metalloenzyme, then converts Ang I to the key component of the RAS, which is angiotensin II (Ang II) an octapeptide. Ang II acts upon two main receptor subtypes Ang II type I (AT₁) and Ang II type II (AT₂) and also upon Ang type IV (AT₄) to bring about the main physiological effects of the RAS, namely, vasoconstriction and increase of BP by altering vascular resistance.⁵ Ang II also inhibits renin secretion by the juxtaglomerular cells acting as a negative feedback mechanism. Despite its important contribution to regulating BP homeostasis, excessive RAS activity and chronic production of Ang II is believed to form the basis of many pathological states. This is because Ang II increases BP and has growth promoting effects that lead to organ damage, particularly in the heart and kidneys.⁶

A number of approaches have been taken to control the RAS and two strategies have focused upon blocking the system by inhibiting ACE and AT₁ receptors. These approaches have led to successful treatments for hypertension and heart failure.⁷ However, ACE inhibitors lead to increased levels of Ang I and increased levels of bradykinin (which can result in cough or rarely life threatening angioedema) and will not suppress the non-ACE-dependent production of Ang II.⁵ AT₁ receptor blockade results in increased levels of Ang II, resulting in stimulation of AT₂ and AT₄ receptors. Due to the fact that the interaction of renin with its substrate is the rate-limiting step in the RAS and that renin's substrate specificity for angiotensinogen is unique, successful renin inhibitors are expected to have

* To whom correspondence should be addressed. Phone: +41 61 6965560. Fax: +41 61 6961163. E-mail: juergen_klaus.maibaum@novartis.com.

[†] Current affiliation: Speedel Experimenta AG, Gewerbestrasse 14, CH-4123 Allschwil, Switzerland.

[‡] Current affiliation: Synergix, Ltd., Technology Park Malha, Building 1, Jerusalem 91487, Israel.

[§] NIBR Discovery Technologies, Lichstrasse 35, WSJ-503.12.08, CH-4056 Basel, Switzerland.

^{||} Current affiliation: Prof. Markus Gruetter, Biochemisches Institut, Winterthurerstr. 190, CH-8057 Zürich, Switzerland.

[⊥] Current affiliation: F.Hoffmann-La Roche Ltd., Pharmaceuticals Division, Grenzacherstrasse 124, CH-4070 Basel, Switzerland.

⁴ Abbreviations: ACE, angiotensin converting enzyme; Ang I, angiotensin I; Ang II, angiotensin II; AT₁, angiotensin II type I receptor; AT₂, angiotensin II type II receptor; AT₄, angiotensin II type IV receptor; BP, blood pressure; CVD, cardiovascular disease; Δ MAP_{max}, maximal change in mean arterial blood pressure; RAS, renin-angiotensin system; rh-renin, recombinant human renin.

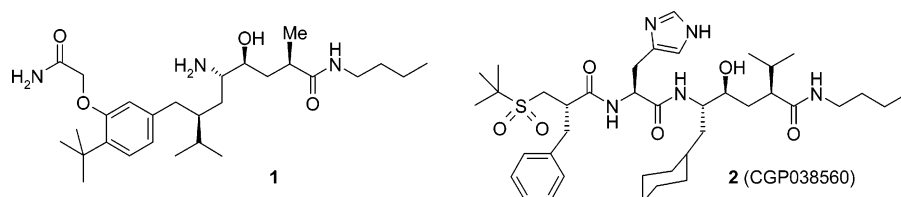
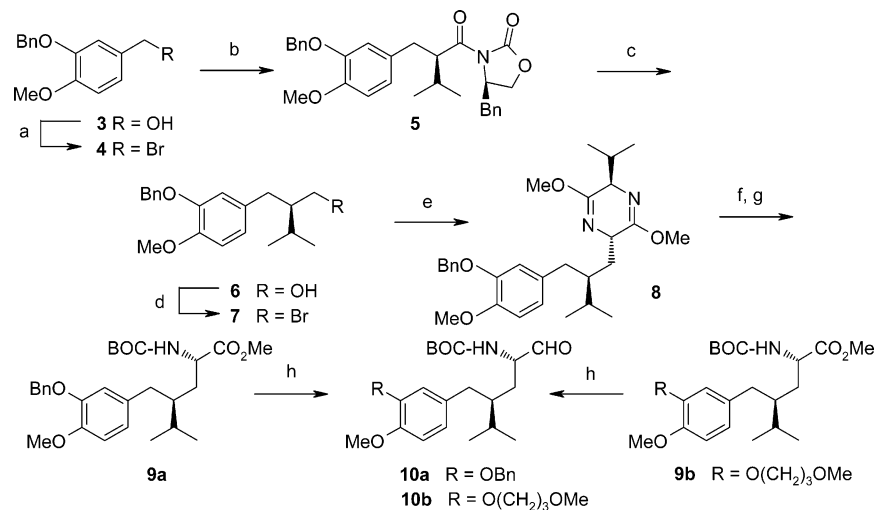


Figure 1. Peptidomimetic inhibitor **1** and previous clinical candidate **2**.

Scheme 1. Synthesis of Aldehyde Intermediates^a



^a Reagents and conditions: (a) Me₃SiBr, CHCl₃, rt, 99%; (b) 4-(*R*)-benzyl-3-isovaleroyl-oxazolidin-2-one, LiHMDS, -75 to 0 °C, 83%; (c) BnSH, *n*-BuLi, THF, 0 °C; then **5**, LiAlH₄, 0 °C, 98%; (d) NBS, Ph₃P, CH₂Cl₂, rt, 93%; (e) (2*R*)-2,5-dihydro-3,6-dimethoxy-2-isopropylpyrazine, *n*-BuLi (1.6 M in hexane), -75 to -20 °C, 94%; (f) 1 N HCl, MeCN; (g) BOC₂O, DIPEA, CH₂Cl₂, 97% (2 steps); (h) DIBAH, toluene, -75 °C (≥97%).

the potential to become “best in class” RAS inhibitors,⁵ as they offer a more selective means for blocking the RAS.⁸

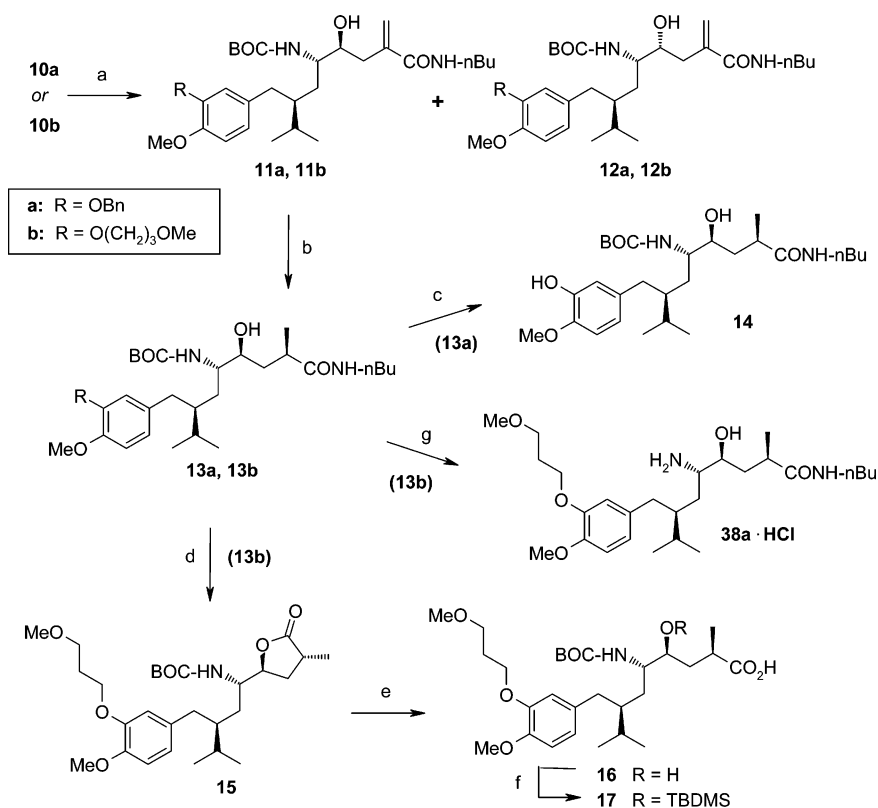
While the attractiveness of renin as a target to inhibit the RAS has been realized for many years, effective strategies to achieve this have not yet progressed beyond phase III clinical trials, despite the numerous approaches toward the design of potent and selective renin inhibitors investigated over more than two decades. Peptide-like renin inhibitors derived from the substrate angiotensinogen amino acid sequence by replacing the scissile peptide bond have been demonstrated to generally exhibit high enzyme specificity, inhibit plasma renin activity, lower BP in marmosets,⁹ and lower BP at least as effectively as ACE inhibitors in human trials.^{10–12} However, the molecular properties and insufficient pharmacodynamic efficacy of these renin inhibitors mimicking the extended β -strand conformation of the renin substrate cleavage fragment have limited their clinical developability.^{13–17} The design of fully nonpeptidic and orally potent renin inhibitors, following a novel target-structure based topological concept, derived from the binding conformation of the peptide-like previous clinical candidate **2** (CGP038560),¹⁸ initially predicted by molecular modeling and subsequently resolved by X-ray crystallography, was recently described by us.^{19–23} This led to the development of several series of unique, low-molecular weight peptidomimetic inhibitors of renin, such as **1**, comprised of a core aminoalcohol transition-state dipeptide isostere, structurally related to the hydroxyethylene mimetic of inhibitor **2**, which is tethered to a combined P3–P1 pharmacophore (Figure 1). It was found that potent inhibition of human renin was related to a hitherto unprecedented binding mode to a distinct nonsubstrate binding site S3^{sp}.²² Exploitation of this previously unrecognized binding site resulted in dramatically increased binding affinity and excellent selectivity against related enzymes of the aspartic protease family. Encouraged by these initial results, and described herein, we have expanded our

studies to identify analogues of this novel compound class, which display improved in vitro potency in the presence of plasma, good oral bioavailability and in vivo efficacy in animal models. Part of this work has been published as a preliminary account²⁴ when we described the discovery of highly potent 5(*S*)-amino-4(*S*)-hydroxy-8-phenyl-octanecarboxamide analogues derived from **1**.

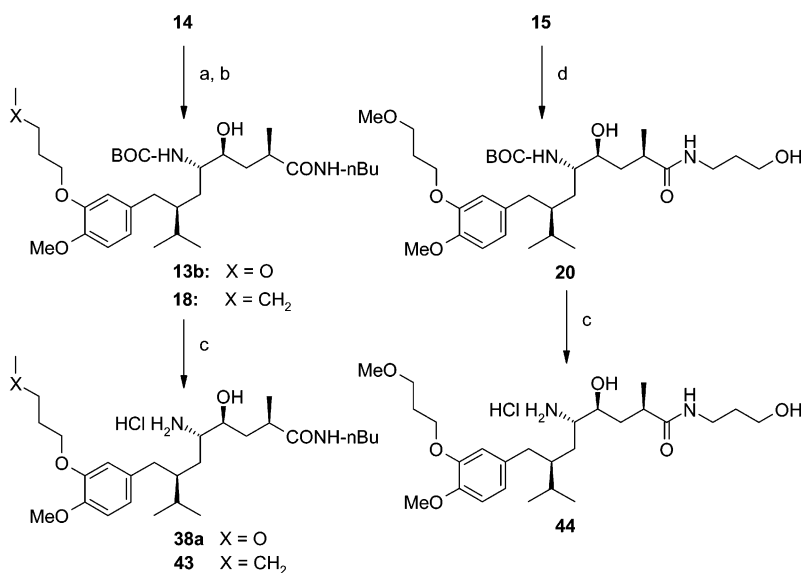
Chemistry

The syntheses of the key intermediates **14** and **15** bearing the transition-state mimetic structural framework was accomplished by a similar route, described by us previously,²⁰ starting from the enantiopure *N*-Boc α -amino aldehydes **10a** and **10b** (Schemes 1 and 2). For efficient structural modification of the *meta*-aryl side chain at a late synthetic stage, the corresponding *O*-benzyl protected amino ester precursor **9a** was prepared by the Schöllkopf method.²⁵ Thus, diastereoselective alkylation of 4-(*R*)-benzyl-3-isovaleroyl-oxazolidin-2-one with benzyl bromide **4** afforded crystalline **5** in 98% yield on large scale (Scheme 1). Cleavage of the auxiliary with benzyl mercaptan/*n*-BuLi followed by LiAlH₄ reduction of the resulting thioester gave the enantiomeric alcohol **6**, which was transformed with NBS/Ph₃P to bromide **7**. The Schöllkopf adduct **8** was obtained by highly diastereoselective alkylation²⁶ to give, after mild acidic hydrolysis and *N*-Boc protection, derivative **9a** in excellent overall yield. DIBAH reduction then afforded crude aldehyde **10a**, and in a similar fashion **10b** from known **9b**,²⁶ which were used in the next reaction step without further purification.

For efficient generation of the dipeptide transition-state mimetic portion, we adapted the protocol by D. J. Kempf²⁷ (Scheme 2). Reaction of aldehyde **10a** with the Li-dianion of *N*-butylmethacrylamide (see Supporting Information) in the presence of Ti(*Oi*-Pr)₃Cl afforded a mixture of **11a/12a** in a

Scheme 2. Synthesis of the Transition-State Mimetics^a

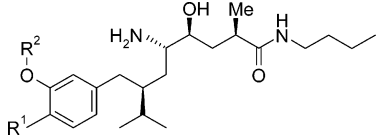
^a Reagents and conditions: (a) *N*-butylmethacrylamide, *n*-BuLi (1.6 M in hexane), Ti(Oi-Pr)₃Cl (1 M in hexane), THF, -78 °C; (b) H₂, MeOH, Ru₂Cl₄[(*S*)-BINAP]₂NEt₃, 20 h, rt, 25 bar; (c) H₂, 5% Pd/C, MeOH, quant.; (d) *p*-TsOH, CHCl₃, rt, 75%; (e) LiOH (1 M in water), 1,2-DME/water 2:1, rt; (f) (1) TBDMSiCl, imidazole, DMF, 6 days, rt; (2) AcOH, THF/water, 68% (2 steps from **15**); (g) 4 N HCl in EtOAc, 0–2 °C, 18 h.

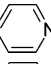
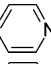
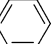
Scheme 3. Synthesis of Inhibitors via *O*-Alkylation or Direct Lactone-Opening^a

^a Reagents and conditions: (a) NaH, MeO(CH₂)₃I, DMF, 86% (**13b**); (b) NaH, *n*-C₅H₁₁I, DMF, rt, 70% (**18**); (c) 4 N HCl/dioxane, 0 °C; (d) NH₂(CH₂)₃OH (neat), 80 °C, 82%.

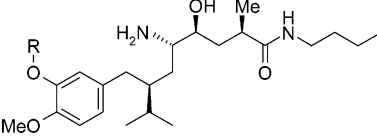
0.7:1 diastereomeric ratio and >60% overall yield, which were separated by repeated silica gel chromatography. Subsequent hydrogenation of the desired 2(*S*)-**11a** using Noyori's (*S*)-BINAP ruthenium catalyst²⁸ afforded 4(*R*)-configured **13a** with high diastereoselectivity (de ≥ 95% by RP-HPLC). The minor 4(*S*)-epimer could be removed by flash chromatography (FC) and recrystallization from EtOAc/hexane to give the single isomer **13a** (mp 124–125.5 °C). Hydrogenation on 10% Pd/C afforded the phenolic **14** as the key intermediate, which allowed,

via *O*-alkylation and final *N*-Boc deprotection with 4 N HCl in dioxane according to Scheme 3, the preparation of the inhibitors listed in Tables 1 and 2. Similarly, the analogous methoxypropoxy derivative **13b** was prepared as a single isomer from **10b** after recrystallization (mp 106.5–107 °C) via a 2:3 ratio of separable **11b** and **12b** and subsequent diastereoselective catalytic hydrogenation of **11b** (Scheme 2). Because we envisaged a broader exploration of the structure–activity relationship related to the P2' position of the new inhibitors,

Table 1. *In Vitro* Activity of Renin Inhibitors with *para*-OMe versus *para*-*t*-Butyl at the P3 Aryl Position^a


| cmpd | R ¹ = | R ² = | binding affinity IC ₅₀ (nM), renin (pH 7.2) | | |
|------------------------|--------------------|---|---|---------------------|---------------------|
| | | | human | | marmoset |
| | | | purified ^b | plasma ^c | plasma ^c |
| 27 ^d | <i>tert</i> -butyl | CH ₂ CO ₂ Me | 6 | 210 | 230 |
| 28 | MeO | CH ₂ CO ₂ Me | 4 | 340 | 190 |
| 1 ^d | <i>tert</i> -butyl | CH ₂ CONH ₂ | 20 | 460 | 230 |
| 29 | MeO | CH ₂ CONH ₂ | 92 | nd ^e | nd |
| 30 | MeO | CH ₂ CONHMe | 42 | 95 | 40 |
| 31 ^d | <i>tert</i> -butyl | CH ₂ SO ₂ Me | 13 | 160 | 230 |
| 32 | MeO | CH ₂ SO ₂ Me | 50 | 220 | 90 |
| 33 ^d | <i>tert</i> -butyl |  | 26 | nd | nd |
| 34 | MeO |  | 5 | 23 | 21 |
| 35 | MeO |  | 0.6 | 13 | 5 |

^a Compounds were obtained as HCl salts according to the General Procedures A or B; see Experimental Section—Biological Materials and Methods. ^b Purified human renin, measured at pH 7.2. ^c Human or marmoset plasma renin assay; see Experimental Section. ^d Reference 20; about a 1:1 mixture of 4(*R*)- and 4(*S*)-configured diastereomers. ^e Not determined.

Table 2. Modification of the P3^{SP} Aryl Side Chain^a


| cmpd | R = | binding affinity IC ₅₀ (nM), renin (pH 7.2) | | |
|-------------------------|--|---|---------------------|---------------------|
| | | human | | marmoset |
| | | purified ^b | plasma ^c | plasma ^c |
| 36 | CH ₂ CH ₂ OMe | 11 | 38 | 15 |
| 37 | CH ₂ CH ₂ OEt | 4 | 32 | 31 |
| 38a | CH ₂ CH ₂ CH ₂ OMe | 1 | 1 | 3 |
| 38b ^d | | 120 | nd ^e | nd |
| 39 | CH ₂ CH ₂ CH ₂ OEt | 3 | 20 | 25 |
| 40 | CH ₂ CH ₂ CH ₂ OH | 6 | 36 | 9 |
| 41 | CH ₂ CH ₂ CH ₂ CH ₂ OMe | 2 | 22 | 18 |
| 42 | CH ₂ CH ₂ OCH ₂ CH ₂ OMe | 19 | 90 | 70 |
| 43 | (CH ₂) ₄ CH ₃ | 4 | 70 | 140 |

^a Compounds were obtained as HCl salts according to the General Procedures A or B; see Experimental Section—Biological Materials and Methods. ^b Purified human renin, measured at pH 7.2. ^c Human or marmoset plasma renin assay; see Experimental Section. ^d 4(*S*)-epimer of **38a**, see Scheme 4. ^e Not determined.

13b was efficiently transformed by the reaction with equimolar *p*-TsOH in CHCl₃ to the corresponding lactone intermediate **15**. Alternatively, alkaline hydrolysis of **15** to the γ -hydroxy acid **16** and subsequent *O*-silylation provided the acid intermediate **17**²⁹ (Scheme 2).

Lactone **15** underwent direct aminolysis in the presence of various amines (neat), as exemplified in Scheme 3. Hence, heating of **15** in aminopropanol at 80 °C afforded intermediate **20** in high yield, which was transformed under standard conditions to the inhibitor **44** as its hydrochloride salt. The standard coupling reaction of carboxylic acid **17** to a number of P'2 amines using (EtO)₂P(O)CN/NEt₃ in DMF, followed by

removal of the *O*-TBDMSi protecting group and final *N*-Boc cleavage (Scheme 4), afforded inhibitors **47**, **48**, **59–62**, **64–69**, and **75–77** (see Tables 3–5). Inhibitor **58** bearing a terminal carboxylic acid at P'2' was prepared from the ethyl ester **22** by alkaline saponification to give **23**, followed by final *N*-Boc cleavage, whereas the corresponding ethyl ester analogue **60** was obtained directly from **22**.

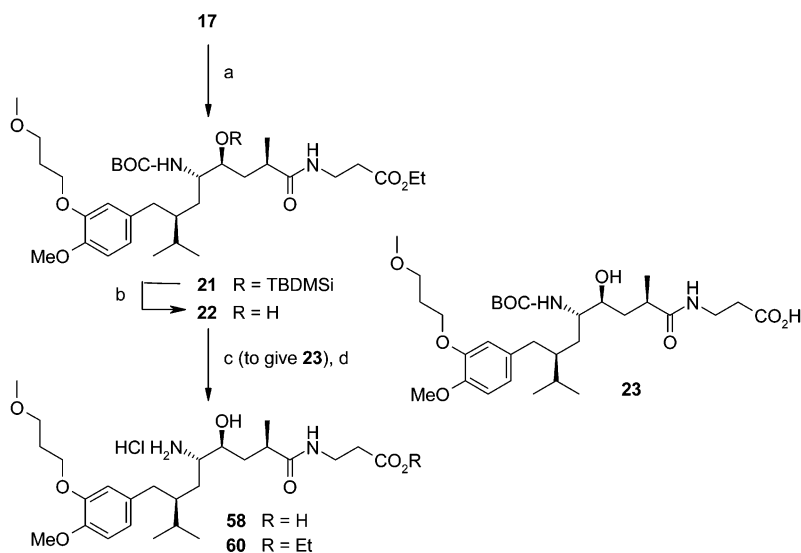
Inhibitor **38a** was initially prepared on a small scale from **14** by *O*-alkylation with 3-methoxy-propyl iodide (Scheme 3) and final *N*-deprotection with 4 N HCl in dioxane. Further preclinical studies then required multigram quantities of this compound, which were more advantageously obtained from intermediate **13b** (Scheme 2) by *N*-Boc deprotection with 4 N HCl in EtOAc at 0–2 °C to afford **38a** as its amorphous monohydrochloride salt in high purity.

The structure and absolute configuration of **13b** was confirmed by single-crystal X-ray analysis (Figure 2). To demonstrate that the 4(*R*) configuration at the P1' position of the dipeptide mimetic portion is required for strong affinity to recombinant human renin (rh-renin) also for this novel class of inhibitors, the 4(*S*)-epimer **38b** was prepared (Scheme 5). The 4(*S,R*)-diastereomeric mixture (ca. 1:1 ratio), obtained from the mother liquors after purification of **13b** by recrystallization, was transformed to the corresponding *N,O*-acetals **24** and **25**, which were readily separated by silica gel chromatography. Stepwise deprotection of **25** gave **26** and, subsequently, the pure 4(*S*)-configured inhibitor **38b** (Table 2). Likewise, transformation of **24** afforded compound **38a**, which was identical with the material obtained as described above.

Results and Discussion

Inhibitor Design Concept. The basic target-structure topographical concept upon which the design of novel chemotype renin inhibitors such as **1** and several related inhibitor series was based has been described in detail previously.^{20,21} Initially, no X-ray crystal complex structures with rh-renin were available to us to probe the enzyme-bound conformation for our prototype lead inhibitors. In particular, the incorporation of H-bonding groups into the combined P3–P1 pharmacophore, targeted toward Ser219 for mimicking a key binding interaction of peptide-like renin inhibitors, turned out to be a promising approach leading to *in vitro* highly potent inhibitors.

Computational docking of inhibitor **1** suggested to us that the large contiguous hydrophobic S3–S1 specificity site of the human enzyme is fully occupied by the complementary hydrophobic P1 isopropyl and the P3 *tert*-butyl groups, respectively.²⁰ Furthermore, the side chain carboxamide tethered to the phenyl spacer was anticipated to be located at a distance that would facilitate H-bonding to the Ser219 backbone NH. In the predicted binding mode, an *N*-alkyl residue would be directed toward the S4 binding site. Accordingly, we considered structural modifications that could mimic the P3–P4 backbone of a classical peptide-like inhibitor with the potential to extend further into the S4 pocket, in an attempt to find more effective renin inhibitors. In the course of this SAR work, we discovered inhibitors such as **38a**, bearing an extended substituent at the aryl spacer position, that showed improved *in vitro* potencies toward rh-renin. Eventually, the X-ray structure of **38a** bound to rh-renin was resolved (*vide infra*)²² and revealed the existence of an unexpected interaction to a distinct binding site extending from the S3 pocket of rh-renin. In addition to this unprecedented binding mode to the nonsubstrate S3^{SP} pocket, the crystal structure also demonstrated that the alkyl ether side chain of **38a** was not interacting directly with Ser219 as initially hypothesized.

Scheme 4. Synthesis of Renin Inhibitors via Amide Coupling to Acid Intermediate 17^a

^a Reagents and conditions: (a) $\text{H}_2\text{N}(\text{CH}_2)_2\text{CO}_2\text{Et}$ (HCl), Et_3N , DMF, $(\text{EtO})_2\text{P}(\text{O})\text{CN}$, rt, 94%; (b) *n*-Bu₄NF (hydrate), DMF, rt, 80%; (c) 1 N NaOH, MeOH, 90%; (d) 4 N HCl/dioxane, 0 °C.

Table 3. In Vitro Activity of Renin Inhibitors with Modified Substitution at the P₂' Position^a

| cmpd | R = | binding affinity IC ₅₀ (nM), renin (pH 7.2) | | |
|------|---|---|------------------------------|---------------------------------|
| | | human purified ^b | human plasma ^c | marmoset plasma ^c |
| 44 | (CH ₂) ₃ OH | 2 | 2 | 2 |
| 45 | (CH ₂) ₃ OMe | 0.4 | 3 | 3 |
| 46 | (CH ₂) ₄ OH | 0.8 | 2 | 2 |
| 47 | (CH ₂) ₂ NMe ₂ | 18 | 12 | 17 |
| 48 | (CH ₂) ₃ NH ₂ | 16 | 37 | 53 |
| 49 | (CH ₂) ₂ -N | 22 | nd | nd |
| 50 | (CH ₂) ₂ -N | 2 | 3 | 7 |
| 51 | (CH ₂) ₂ -N | 2 | 8 | 29 |
| 52 | CH ₂ -N | 2 | 3 | 4 |
| 53 | (CH ₂) ₃ -N | 11 | 10 | 7 |
| 54 | (CH ₂) ₂ -N | 2 | 10 | 12 |
| 55 | (CH ₂) ₂ -N | 2 | 7 | 11 |
| 56 | (CH ₂) ₂ -N | 10 | 7 | 52 |
| 57 | (CH ₂) ₂ -N | 5 | 15 | 49 |

^a Compounds were obtained as HCl salts according to the General Procedures A or B; see Experimental Section—Biological Materials and Methods. ^b Purified human renin, measured at pH 7.2. ^c Human or marmoset plasma renin assay; see Experimental Section.

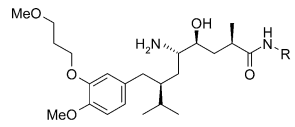
In Vitro Biological Data and Structure–Activity Relationships. Modification of the P₃ Aryl Substitution. Inhibitors **1**, **27**, and **31** bearing a lipophilic *tert*-butyl residue at P₃ showed high affinity to purified human renin in a buffer assay at pH 7.2, but were found to be only poor inhibitors of both human

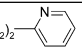
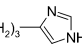
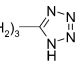
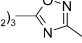
Table 4. In Vitro Activity of Renin Inhibitors with Modified Substitution at the P₂' Position^a

| cmpd | R = | binding affinity IC ₅₀ (nM), renin (pH 7.2) | | |
|-----------|--|---|------------------------------|---------------------------------|
| | | human purified ^b | human plasma ^c | marmoset plasma ^c |
| 58 | (CH ₂) ₂ CO ₂ H | 12 | 17 | 23 |
| 59 | (CH ₂) ₃ CO ₂ H | 3 | 10 | 13 |
| 60 | (CH ₂) ₂ CO ₂ Et | 4 | 11 | 13 |
| 61 | (CH ₂) ₃ CO ₂ Me | 1 | 2 | 3 |
| 62 | (CH ₂) ₄ OCOMe | 6 | 36 | 9 |
| 63 | (CH ₂) ₃ CN | 1 | 3 | 3 |
| 64 | (CH ₂) ₂ CONH ₂ | 7 | 17 | 13 |
| 65 | (CH ₂) ₃ CONH ₂ | 1 | 3 | 11 |
| 66 | (CH ₂) ₃ CONHMe | 3 | 2 | 11 |
| 67 | (CH ₂) ₃ CONH(CH ₂) ₂ OMe | 2 | 4 | 10 |
| 68 | (CH ₂) ₄ CONH ₂ | 2 | 1 | 9 |
| 69 | (CH ₂) ₃ CO-N | 2 | 2 | 4 |
| 70 | (CH ₂) ₂ NHCOMe | 0.3 | 20 | 18 |
| 71 | (CH ₂) ₂ SO ₂ Et | 4 | 16 | nd ^d |
| 72 | (CH ₂) ₃ SO ₂ tBu | 6 | 7 | 25 |
| 73 | (CH ₂) ₂ SO ₂ NMe ₂ | 2 | 5 | 9 |

^a Compounds were obtained as HCl salts according to the General Procedures A or B; see Experimental Section—Biological Materials and Methods. ^b Purified human renin, measured at pH 7.2. ^c Human or marmoset plasma renin assay; see Experimental Section. ^d Not determined.

and marmoset renin in a modified in vitro enzyme assay in the presence of plasma (Table 1). Marked reductions of in vitro potencies in the presence of plasma have been reported for renin inhibitors from different structural classes, which could be due to interference with plasma components, rendering these inhibitors significantly less effective in vivo.³² Renin binding affinity in the presence of plasma can be affected, at least in part, by the lipophilicity of the compound, and large potency discrepancies are often observed for highly hydrophobic inhibitors.^{33,34} We, therefore, reasoned that replacing the highly lipophilic *tert*-

Table 5. In Vitro Activity of Renin Inhibitors with Modified Substitution at the P2' Position^a


| compd | R = | binding affinity IC ₅₀ (nM), renin (pH 7.2) | | |
|-------|---|---|---------------------|---------------------|
| | | human | | marmoset |
| | | purified ^b | plasma ^c | plasma ^c |
| 74 |  | 8 | 14 | 16 |
| 75 |  | 4 | 5 | 7 |
| 76 |  | 3 | 4 | 7 |
| 77 |  | 2 | 3 | 15 |

^a Compounds were obtained as HCl salts according to the General Procedures A or B; see Experimental Section—Biological Materials and Methods. ^b Purified human renin, measured at pH 7.2. ^c Human or marmoset plasma renin assay; see Experimental Section.

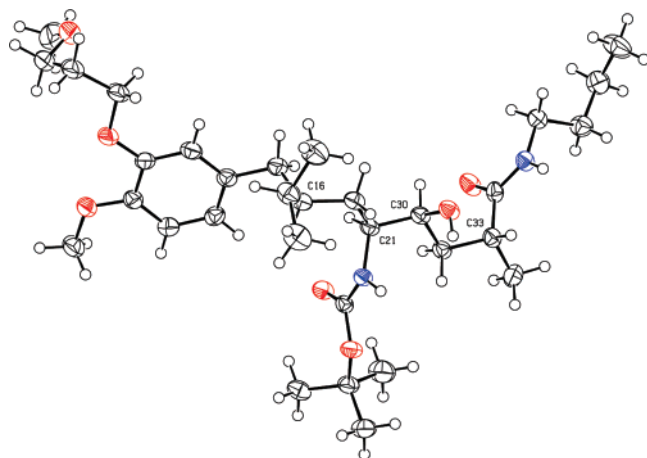


Figure 2. Structure of compound **13b** in the crystal (atomic displacement ellipsoids drawn at the 50% probability level, hydrogen atoms drawn as spheres of arbitrary radius³⁰). For the enantiomer shown (C16S, C21S, C30S, C33R), the Flack *x* parameter is refined to 0.01(11).³¹

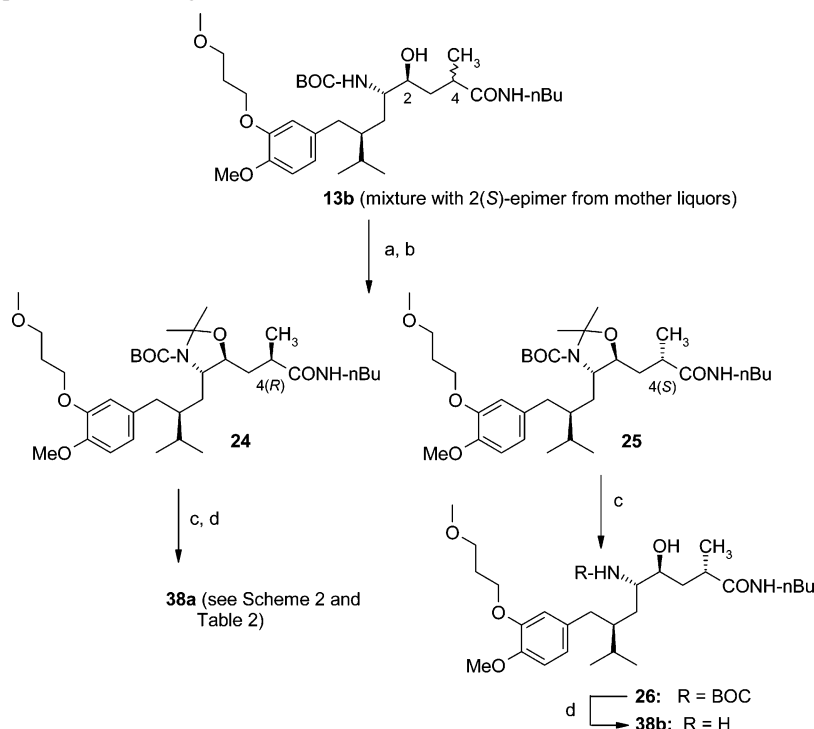
butyl by smaller and more polar residues would increase potencies of the new chemotype inhibitors under more physiologically relevant in vitro assay conditions.

Several inhibitors bearing a less lipophilic *para*-methoxy group at the putative P3 position were prepared from readily available starting materials (vide supra) and were shown to have very similar in vitro affinities toward purified renin as compared to their respective *tert*-butyl analogues (Table 1). As noted previously,²⁰ replacement of the terminal carboxylic ester of highly potent inhibitor **28** by a carboxamide (**29** and **30**) or a sulfone (**32**) as H-bond acceptors caused a drop in binding affinity up to 20-fold. Intriguingly, the OMe analogues **36** and **38** exhibited only slightly lower IC₅₀ values toward human and marmoset plasma renin. The considerably reduced potency of **28** in the presence of plasma was attributed to potential ester cleavage under the assay conditions. Surprisingly, the most potent inhibitor in this series was the benzyloxy derivative **35** with subnanomolar IC₅₀ in the buffer assay, albeit with slightly lower affinity in plasma. The 4-pyridyl analogue **34**, designed to potentially interact with Ser219, showed a remarkable 10-fold lower affinity toward renin, as compared to **35**, thus

indicating that a H-bonding functionality was not necessarily required at this position for strong binding to the enzyme (vide infra).

Variation of the Tethered P3 Aryl Side Chain. In line with our results from SAR studies on related topographical renin inhibitors,²¹ substitution of the phenyl spacer with various alkyl ether and hydroxylated alkyl residues ortho to the OMe group at the P3 site, afforded a series of highly potent in vitro analogues **36–43**, as represented in Table 2. The influence of varying the length of the linear chain from five up to eight atoms, as well as the position of the oxygen atom along the chain, was extensively investigated. As discussed above, we again placed particular emphasis upon producing inhibitors that demonstrated high binding affinities to human renin, which were also retained in the presence of plasma, as a key requirement for in vivo potency. This turned out to be one of the major challenges during lead optimization, because such discrepancies in binding affinities were dependent on even minor structural changes. This is most strikingly illustrated by a comparison of the in vitro data of inhibitor **38a**, bearing a terminal methyl ether group, with that of the *n*-pentyloxy-substituted inhibitor **43** of the same chain length. Both compounds were equipotent in the buffer assay, however, **43** showed a greater than 20-fold loss in potency against primate plasma renin, whereas compound **38a** retained its low-nanomolar binding affinity under the physiological assay conditions. Furthermore, a shift in the position of the ether oxygen, as in **37**, or extension of the side chain by one carbon (**39** and **41**) provided similar binding affinities in buffer, but caused a significant, albeit less dramatic, increase in IC₅₀ values when determined in plasma. The terminal OH group in **40** slightly reduced the in vitro affinity, particularly against human plasma renin. Inhibitor **36**, with a shorter substituent, was less active, as was **42**, bearing a further extended and highly flexible side chain. The 4(*S*)-configured P1' epimer **38b** was more than 50-fold less active than 4(*R*)-**38a** against rh-renin.

In Vitro SAR of P2' Moiety. With the methoxypropoxy side chain of inhibitor **38a** as the optimal P3^{SP} ligand in hand, we next turned to the extensive variation of the P2' position, with the aim of identifying compounds with equally high or further improved affinities to primate plasma renin, as well as of high in vivo oral potency in sodium-depleted marmosets. Previously, the C-terminal P2' pharmacophore of hydroxyethylene dipeptide isostere renin inhibitors has been shown to be less sensitive toward structural modifications, thus allowing the incorporation of a variety of functional groups to tune their physicochemical properties.^{35,36} A broad range of analogues bearing neutral (inhibitors **44–46**, **60–73**), basic (**47–57**), or acidic (**58**, **59**, **76**) functional groups, as well as heteroaryl residues (**74**, **75**, **77**), tethered by a two- to four-carbon spacer to the dipeptide isostere carboxamide were examined. Tables 3–5 summarize the in vitro IC₅₀ data against human (buffer and plasma assay) and marmoset plasma renin. In general, low nanomolar binding affinities toward buffered renin were determined for most inhibitors, with the methyl ether derivative **45** and the inversed acetamide **70** being the most potent analogues. A marked decrease in the binding affinity of greater than 10-fold as compared to **38a** was observed only for a few analogues, in particular for amines **47–49** (Table 3). Interestingly, incorporation of a heteroatom into the piperidine ring of **49** restored high affinity to the enzyme (e.g., **50–52**, **54–55**), whereas hydroxylation at the 4-position was less effective (**56**, **57**). Table 4 presents inhibition data for carboxylic ester (**60–62**), nitrile (**63**), carboxamide (**64–70**), sulfone (**71**, **72**), and sulfonamide (**73**)

Scheme 5. Synthesis of Epimeric 2(*S*)-Configured Inhibitor **38b**^a

^a Reagents and conditions: (a) 2,2-DMP, *p*-TsOH (hydrate), CH₂Cl₂, rt (quant.); (b) separation by silica gel chromatography; (c) *p*-TsOH (hydrate), MeOH, rt (72% for **26**); (d) 4 N HCl/dioxane, 0 °C (quant.).

derivatives, demonstrating that these functionalities are well accommodated at the P2' position. The carboxylic acid **59** was of equivalent potency, as was the tetrazole **76** (Table 5), whereas a minor drop in affinity was seen for acid **58** bearing a shorter 2-carbon spacer. All new renin inhibitors were found to be highly selective against porcine pepsin and bovine cathepsin D (no inhibition at 10 μM concentrations; data not shown).⁹

As discussed above, retention of high affinity of inhibitors in the presence of plasma was considered as a key requirement. With the striking exception of the acetamide **70** and, to a lesser extent, the alkylether **45**, all of the inhibitors listed in Tables 3–5 exhibited similar or only slightly reduced (less than 5-fold) potencies in the presence of plasma. We were gratified that a number of analogues from this series were identified that revealed single-digit nanomolar IC₅₀ values toward human plasma renin, such as alcohols **44** and **46**, the P2' morpholines **50** and **52**, and, in particular, inhibitors **65–69** bearing a terminal primary, secondary or tertiary amide group. There was, though, a trend for a slightly reduced in vitro affinity toward marmoset renin for some of these analogues when measured under plasma assay conditions.

The generally very low discrepancies in IC₅₀s against purified buffer versus plasma renin could be attributed, at least in part, to a favorable physicochemical profile of these inhibitor molecules, which is in general characterized by very high intrinsic aqueous solubility and high solubility in acidic buffer, as well as a relatively low lipophilicity range. For example, inhibitor **38a** as its HCl salt showed a reasonably low *n*-octanol/water coefficient logP = 1.96 at pH 7.4 and remarkably high solubility of 11.0 g/L at neutral pH in phosphate buffer (22 °C) and of 56 g/L at pH 6.0, with a pK_a of 9.13. In this respect, this structurally novel class of renin inhibitors clearly differs from the previous peptide-like inhibitors, such as **2**, which were in many cases of high lipophilicity and poor solubility, hence limiting their overall pharmacokinetic properties.

X-ray Structure of rh-Renin with 38a. In the course of our SAR work, the crystal structure of rh-renin soaked with inhibitor **38a** was determined at 3.1 Å resolution (Figures 3 and 4).²² The overlay of enzyme-bound **38a** with the cocystal conformation of the peptide-like inhibitor **2** revealed an overall good agreement of the positioning of the dipeptide transition-state mimetic encompassing the P1'–P2' portion, as well as a tight occupancy of the large contiguous S1–S3 specificity pocket of rh-renin. Hence, the bulky P1 isopropyl of **38a** deeply penetrates into the hydrophobic S1 pocket, whereas the small *para*-methoxy group of the phenyl spacer appears to sufficiently fill the complementary S3 site, with the Me group pointing toward Leu114, Ala115, and Phe117. In contrast to the transition-state mimetic OH group of inhibitor **2**, which forms a H-bond network with both Asp32 and Asp215, the dipeptide isostere OH of **38a** adopts a shifted position and interacts only with Asp32 (distances to the outer oxygen atom 3.1 Å, and inner oxygen atom 3.0 Å, respectively). Furthermore, it is interesting to note that the basic NH₂ of **38a** is not within H-bond distance to any of the two aspartates, but instead forms a H-bond to the backbone carbonyl of Gly217 (3.0 Å), similar to the interaction observed for the P2–P1 carboxamide NH of the peptidic inhibitor **2** (Figure 3).²² As a consequence of the slight positional shift and minor conformational changes of the dipeptide isostere of **38a** (as compared to **2**), the P1' Me group is occupying its complementary site only suboptimally. The adjacent amide carbonyl still can form a H-bond to Gly77 important for strong binding, due to a conformation adaptation of the flexible enzyme flap loop, which positions the aliphatic butyl chain into the S2' pocket (Figure 4).

Surprisingly, and deviating from the original design concept based on modeling considerations (vide supra), the X-ray structure of **38a** revealed the very close fit of the methoxypropoxy side chain to a distinct, narrow nonsubstrate pocket, which extends from the S3 site perpendicular to the axis of the enzyme

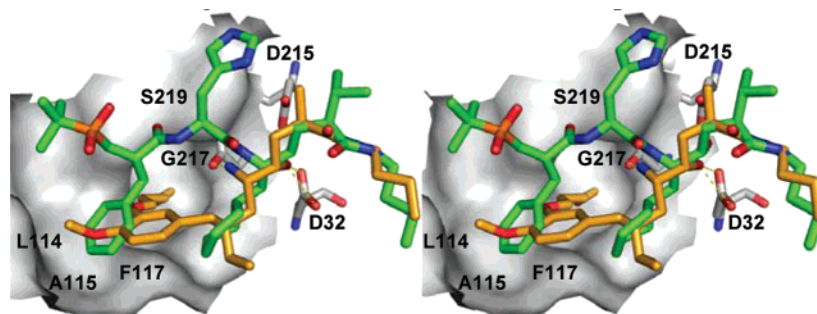


Figure 3. Stereoview with the super-positioned X-ray crystal structures of the peptide-like inhibitor **2** (green color)³⁸ and the nonpeptide inhibitor **38a** (orange color) complexed to rh-renin. Inhibitors are shown in ball-and-stick model, with oxygen and nitrogen atoms in red and blue, respectively. The catalytic aspartic acids (Asp32 and Asp215) as well as Gly217 are shown as stick model in gray color. H-bond interactions between **38a** and Asp32 and Gly217 are shown as dotted yellow lines. The S3 and S3^{sp} pockets are shown as a solvent accessible surface in gray. The graphs in Figures 3 and 4 were generated using the PyMOL software package.³⁷

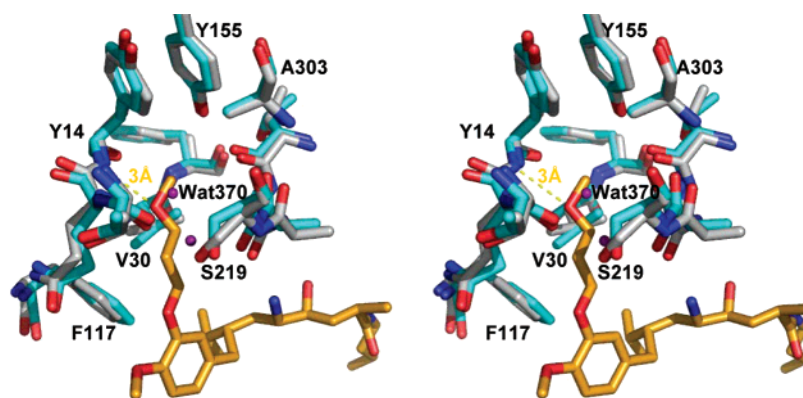


Figure 4. Stereo picture with close-up view of the amino acids (in blue) comprising the S3^{sp} subpocket of rh-renin accommodating the methoxypropoxy side chain of inhibitor **38a**. Superimposed are the same amino acids (gray) flanking the S3^{sp} pocket of rh-renin in complex with **2**. The two water molecules 370 and 410 (magenta spheres) were observed in the X-ray complex with **2** only.

cleft and which is flanked by Tyr14, Tyr155, Val30 and Ala303 (Figure 3). Furthermore, no direct binding interaction to Ser219 is observed for **38a** in its complex structure (the distances of the Ser219 hydroxyl to the ligand side chain ether oxygens were found to be 5.4 and 4.7 Å, respectively). The terminal ether oxygen of the inhibitor tightly interacts with the backbone nitrogen of Tyr14 (Figure 4, dotted yellow line) and replaces the two water molecules W370 and W410 bound in the complex structure with the peptide-like inhibitor **2** and similarly in the crystal structure of apo-rh-renin.³⁸ This H-bond is likely to be a favorable interaction as it is within a binding site completely shielded from solvent space.³⁹ On the other hand, this interaction appeared not to be essential for strong binding, as demonstrated by the similar in vitro potency of inhibitor **43** bearing an all-carbon chain of the same length. No attempts were made to obtain an X-ray structure of renin-bound **43**, as the common binding mode of several related inhibitors from different sub-series and with modified side-chains suggested a very similar positioning of the respective side chains of **38a** and **43** within the S3^{sp} site.²² Shortening of the side chain by one carbon, as for **36**, reduced the binding affinity 10-fold, which could be restored by adding one terminal carbon atom (**37**), again emphasizing the importance of hydrophobic interactions for potent ligand affinity. Extending the side chain further (**42**) would force the inhibitor to adopt a disfavored conformation due to the limited depth of the rigid S3^{sp} pocket of about 9 Å, hence resulting in a markedly weaker inhibitor. The amino acids flanking the S3^{sp} site undergo at most very minor conformational changes upon binding of **38a** to the active site of rh-renin (Figure 3). This is in line with results we have obtained with inhibitors from other series,^{21–24} indicating that this is a rather rigid pocket

of limited size. Still, this channel can accommodate a suitably positioned phenyl residue of an inhibitor molecule as shown previously by X-ray;²² retrospective computational docking of the benzyloxy inhibitor **35** suggested a similar binding mode by interacting with the S3^{sp} pocket (data not shown), which would explain its strong binding affinity. The independent discovery,^{33,40–42} and exploitation for potent inhibitor design^{43–45} of this nonsubstrate binding site by other groups was disclosed after we had completed our structure-based design work.

In Vivo Activity in Conscious Telemetered Na⁺-Depleted Marmosets. The oral potency of inhibitors that demonstrated high in vitro affinities for human and marmoset plasma renin was evaluated in conscious telemetered sodium-depleted and normotensive marmosets by constantly measuring the effect on systolic, diastolic, and mean arterial blood pressures (MAPs) and heart rate.⁴⁶ Time courses of changes (Δ) in MAP values from baseline for the test compounds and vehicle were compared. In addition, the plasma renin activity was determined 1.5, 3, 6, and 24 h post-dosing in nontelemetered marmosets. Table 6 summarizes the results for selected inhibitors. Compounds **45**, **52**, **54**, and **65** showed a rapid onset of action and exhibited significant reductions of Δ MAP at peak (1–2 h after dosing); however, the duration of action was relatively short for these compounds, with Δ MAP recovering to vehicle-treated baseline values within 5 h post-dose. Compound **66**, a very close analogue of **65** (Table 4), with a terminal P2' N–Me carboxamide, showed a similar Δ MAP lowering effect but a significantly longer duration of action of up to 7 h. The carboxylic ester analogue **61** showed only a very minor and short-lasting

Table 6. In Vivo Oral Potency, Duration of Action on Mean Arterial Blood Pressure (MAP), and Inhibition of Plasma Renin Activity (PRA) of Selected Renin Inhibitors in Na⁺-Depleted Marmosets

| compd | single oral dose ^a (mg/kg) | peak ΔMAP ^b (mmHg) | duration of action ^c (hrs) | % inhibition of PRA at 6 h ^d |
|------------|---------------------------------------|-------------------------------|---------------------------------------|---|
| 38a | 3 | -9 | 8 | 98 |
| 45 | 3 | -21 | 5 | 90 |
| 52 | 10 | -24 | 4 | 88 |
| 54 | 3 | -26 | 3 | 28 |
| 59 | 3 | inactive | | |
| 61 | 3 | minor | <1 | |
| 65 | 3 | -22 | 2 | 95 |
| 66 | 3 | -17 | 7 | 74 |

^a Compounds were administered by oral gavage as clear solutions of their HCl salts in 5% glucose. ^b Maximal ΔMAP: change in mean arterial blood pressure relative to pretreatment period values, reported as the mean of $n > 4$ animals. ^c Time until ΔMAP values returned to baseline levels after oral dosage. ^d PRA: plasma renin activity (see Experimental Section for details).

effect, which was attributed to rapid metabolic ester cleavage in plasma to the corresponding acid **59** being completely inactive orally.

The most potent inhibitor in this series was **38a**, with a long duration of action on MAP of up to 8 h and with plasma renin activity fully blocked at least 6 h after dosing. For compounds **45**, **52**, **65**, and **66**, plasma renin activity was inhibited by more than 74% during at least 6 h following oral administration, whereas during this period ΔMAP returned to baseline. The dissociation between pharmacodynamic effects and ex vivo plasma renin activity measurements might be explained by displacement of the fraction of inhibitor bound to plasma protein under the in vitro assay conditions, leading to a higher free fraction of the inhibitor and, hence, an overestimation of renin inhibition.⁴⁷ Alternatively, the trapping assay, although more appropriate to measure plasma renin activity compared to a conventional assay,⁴⁸ may still overestimate the effectiveness of the compound ex vivo, as plasma Ang I could not be fully protected from degradation. Furthermore, the recovery of BP to baseline observed in vivo could be mediated by an extraplasmatic pool of renin that is not readily accessible to inhibitors and is playing an important role in the control of systemic BP.⁴⁹

Oral administration of single doses of **38a** (1–30 mg/kg, HCl salt in 5% glucose) caused dose-dependent reductions of ΔMAP in sodium-depleted telemetered marmosets (Figure 5). At the 1 mg/kg threshold dose, the peak effect was only moderate and transient, with BP recovering to baseline levels after 4 h. A more pronounced efficacy and a longer duration of action was observed at the 3 mg/kg dose, and a maximum fall in ΔMAP of ~20–25 mmHg (compared with vehicle control) was achieved at the 10 mg/kg dose. With the higher 30 mg/kg dose of **38a**, the magnitude of the MAP reduction did not further increase, however, its duration markedly increased, with significant effects observed even 24 h after dosing. No significant effects on heart rate were observed at any given doses of **38a**. The ΔMAP lowering was paralleled by the inhibition of plasma renin activity, which was completely blocked over the 24 h period after administration of the 10 and 30 mg/kg doses.

The absolute oral bioavailability for **38a** in marmosets was 16%, as estimated from plasma inhibitor concentrations (and possibly of any circulating potent in vivo metabolites) after 3 mg/kg intravenous and 10 mg/kg oral administration by using a renin activity assay.⁵⁰ The terminal elimination half-life $t_{0.5}$ for **38a** was 2.0 ± 0.06 h, with biphasic elimination kinetics (first distribution–elimination phase followed by a second elimination phase). The steady-state volume of distribution was

$V_{dss} = 0.6$ L/kg, which is greater than the expected blood volume, suggesting an extravascular distribution, and plasma clearance CL_p was 5.2 ± 0.4 mL/min/kg. The weaker oral potencies of related inhibitors **45**, **52**, **65**, and **66** in the Na⁺-depleted marmoset model, as compared to **38a**, could be attributed to reduced oral plasma exposures of the respective inhibitors in nondepleted marmosets (preliminary data, not shown), suggesting a limited oral bioavailability for these compounds in monkeys.

Conclusions

The optimization of the P3 and P3^{SP} regions of novel nonpeptide transition state isosteres with an all-carbon 8-phenyl-octanecarboxamide framework, described herein, has provided inhibitors with high in vitro potencies for human and marmoset renin. Importantly, high binding affinities were retained in the presence of plasma, and this was seen as a key requirement to produce inhibitors exhibiting high affinities in vivo. The retention of such affinities was demonstrated using a modified in vitro assay. These new inhibitors are highly soluble in aqueous buffer, in contrast to peptide-based inhibitors that exhibit high lipophilicity and poor aqueous solubility, thus limiting pharmacokinetic properties. Determination of the X-ray structure of the rh-renin/**38a** complex revealed a close interaction of the MeO(CH₂)₃O residue with the previously discovered S3^{SP} pocket, proving the latter to be a common binding site for different series of tethered P3–P1 topographical renin inhibitors. We have discovered a similar, hitherto unprecedented, binding mode for several other (P3–P1)-tethered transition-state mimetic renin inhibitors and have used this structural information to further optimize their in vitro potencies.^{21,22}

For the first time, high in vivo potency has been demonstrated for this novel class of renin inhibitors. In particular, inhibitor **38a** (HCl salt, CGP054061A) induced in a dose-dependent manner (over the range of 1 to 30 mg/kg single dose) a pronounced BP reduction after oral administration to telemetered Na⁺-depleted normotensive marmosets, which was shown to be specifically induced by inhibition of plasma renin. Compound **38a** and related analogues are physico-chemically characterized by their low lipophilicity (logP) and remarkably high intrinsic solubility in water, in contrast to previous peptide-like inhibitors. Absolute oral bioavailability of **38a** was still found to be moderate (16%) in non-depleted marmosets, indicating that other multiple factors may play a role in limiting bioavailability of this novel compound class. Overall, these encouraging results stimulated continued efforts toward the design of more potent in vivo analogues with even greater oral bioavailability.⁵¹

Experimental Section

General methods for experimental and analytical procedures can be found in the Supporting Information. Synthetic amine P2' building blocks were either commercially available, or were prepared according to literature protocols, if not otherwise indicated.

2-Benzyloxy-4-bromomethyl-1-methoxy-benzene (4). To a solution of benzylic alcohol **3** (59.5 g, 0.244 mol)⁵² in CHCl₃ (0.8 L) was rapidly added Me₃SiBr (47.2 mL, 0.365 mol) in a dropwise manner at ambient temperature. After stirring for 15 min, the reaction mixture was concentrated under reduced pressure. The pale-colored solid was dissolved in warm EtOAc (200 mL), followed by the addition of hexane (150 mL) and submission of the mixture to a silica gel column (500 g silica gel) to give, after washing with EtOAc/hexane (1:3) and evaporation of solvent, compound **4** (74.4 g, 99%) as a beige solid [**Caution:** any contact of this material with metal equipment (eg., spatula) should be avoided to prevent rapid decomposition]: mp 95–97 °C (lit. [ref 1] mp 94.5 °C); ¹H NMR (300 MHz, CDCl₃) δ 3.85 (s, 3H), 4.43 (s, 2H), 5.13 (s,

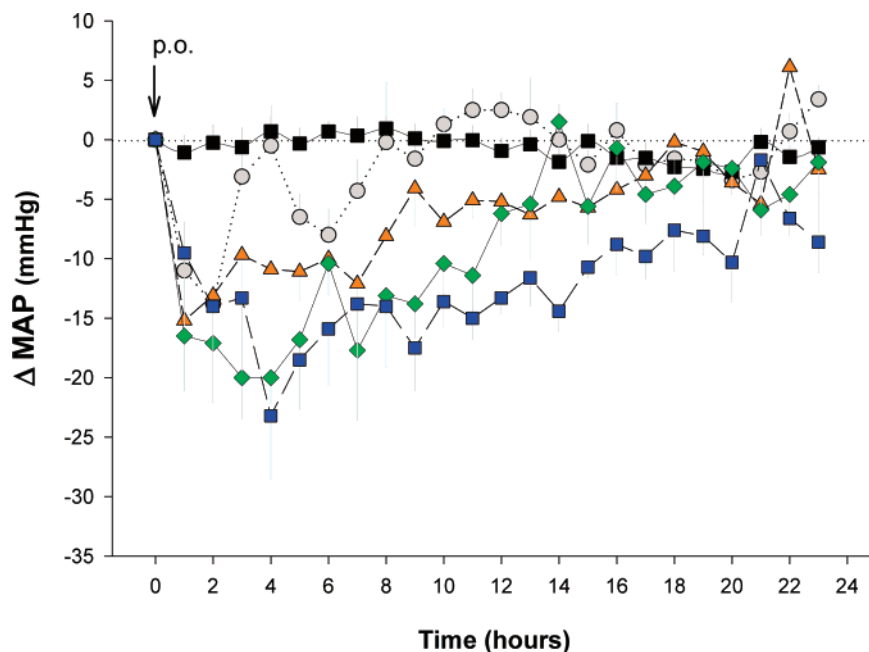


Figure 5. Values are means \pm SEM of the change (Δ) in MAP from baseline over 24 h after p.o. dosing (time 0) with inhibitor **38a**, 1 mg/kg ($n = 4$; gray circles), 3 mg/kg ($n = 4$; orange triangles), 10 mg/kg ($n = 5$; green diamond square), 30 mg/kg ($n = 4$; blue square), or vehicle control ($n = 20$; black square) to Na^+ -depleted freely moving telemetered marmosets. Mean baseline arterial blood pressure and heart rate values in all groups were similar to 81 ± 2 mmHg and 205 ± 8 beats/min observed in the 10 mg/kg p.o. dose group.

2H), 6.8–7.0 (m, 3H), 7.25–7.5 (m, 5H). This material was used in the next step without further purification.

(2S,4R)-4-Benzyl-3-[2-(3-benzoyloxy-4-methoxy-benzyl)-3-methyl-butyl]-oxazolidin-2-one (5). To a 1 M solution of LiHMDS in dry THF (291 mL, 0.291 mol), cooled to -75°C , was added dropwise a solution of 4(*R*)-benzyl-3-isovaleroyl-oxazolidin-2-one (76.0 g, 0.291 mol) in THF (0.9 L). After stirring for 1 h, a solution of **4** (74.4 g, 0.242 mol) in THF (250 mL) was added dropwise at -70°C . The reaction temperature was gradually raised from -70 to 0°C over 2 h, and stirring was continued for 18 h at 0°C . Then, a 10% aqueous NH_4Cl solution (115 mL) was added with cooling and volatiles were removed under reduced pressure. The residue was partitioned between Et_2O and water, and the aqueous layer was extracted with Et_2O . The combined organics were washed with brine and dried (MgSO_4), and the residue was purified by FC (EtOAc/hexane 1:5) to yield **5** (97.6 g, 83%) as white solid: mp 90 – 92°C ; TLC $R_f = 0.25$ (EtOAc/hexane 1:5); HPLC t_R 22.0 min; $[\alpha]_D^{20} -13.6 \pm 1.0$ (c 1.0, CH_2Cl_2); IR (CH_2Cl_2) 3050, 2962, 1589, 1453, 1442, 1158, 1101, 807; $^1\text{H NMR}$ (200 MHz, CDCl_3) δ 1.02 (t, $J = 6$, 6H), 2.0 (m, 1H), 2.18 (m, 1H), 2.7–3.0 (m, 3H), 3.78 (s, 3H), 4.02 (m, 2H), 4.25 (m, 1H), 4.60 (m, 1H), 5.10 (s, 2H), 6.7–7.0 (m, 5H), 7.15–7.45 (m, 8H). Anal. ($\text{C}_{30}\text{H}_{33}\text{NO}_5$) C, H, N.

(2S)-2-(3-Benzoyloxy-4-methoxy-benzyl)-3-methyl-butan-1-ol (6). To a solution of benzyloxy-mercaptane (22.1 mL, 0.188 mol) in dry THF (200 mL), cooled to 0°C , was added dropwise 1.6 M *n*-BuLi in hexane (88 mL, 0.141 mol) over 10 min. To the mixture was then dropwise added **5** (45.8 g, 0.094 mmol) in THF (200 mL). Stirring was continued at 0°C for 1 h, followed by the addition of a precooled (0°C) suspension of LiAlH_4 (14.2 g, 0.376 mol) in THF (0.8 L). After reaction for 2 h at 0°C , EtOAc (52 mL) was added dropwise to the mixture at 0°C , which was stirred for 10 min before adding a 1:1 mixture of THF–water (112 mL; **Caution:** vigorous gas evolution), followed by subsequent addition of 2 N H_2SO_4 (790 mL), water and Et_2O . After separation of the layers, the aqueous phase was extracted with Et_2O , and the combined organics were washed with water, dried (Na_2SO_4), and concentrated. FC purification (EtOAc/hexane 1:4) yielded **6** (29.0 g, 98%) as an oil: TLC $R_f = 0.18$ (EtOAc/hexane 1:3); HPLC t_R 19.0 min; $[\alpha]_D^{20} +6.2 \pm 1.8$ (c 0.55, CHCl_3); IR (CH_2Cl_2) 3618, 2958, 1588, 1514, 1464, 1369, 1232, 1139, 1028; $^1\text{H NMR}$ (300 MHz, CDCl_3) δ 0.92 (d, $J = 8$, 6H), 1.52 (m, 1H), 1.55 (s, 1H), 1.76 (m, 1H), 2.40 (dd, $J = 10$, 15, 1H), 2.60 (dd, $J = 10$, 15, 1H),

3.43 (t, $J = 6$, 2H), 3.86 (s, 3H), 5.17 (s, 2H), 6.7–6.85 (m, 3H), 7.25–7.45 (m, 5H). Anal. ($\text{C}_{20}\text{H}_{26}\text{O}_3$) C, H.

(2S)-2-Benzoyloxy-4-(2-bromomethyl-3-methyl-butyl)-1-methoxy-benzene (7). To a solution of **6** (61.4 g, 0.195 mol) in dry CH_2Cl_2 (1.2 L) was added Ph_3P (61.4 g, 0.234 mol) and, subsequently, NBS (41.6 g, 0.234 mol) in portions at 0 to 10°C . After stirring for 18 h at ambient temperature, the mixture was concentrated and the residue was purified by FC (EtOAc/hexane 1:4) give **7** (68.7 g, 93%) as pale colored solid: mp 61.5 – 63°C ; TLC $R_f = 0.56$ (EtOAc/hexane 1:3); HPLC t_R 24.0 min; IR (CH_2Cl_2) 2960, 1588, 1464, 1442, 1386, 811; $^1\text{H NMR}$ (CDCl_3) δ 0.9–1.0 (2d, 6H), 1.50 (m, 1H), 1.78 (m, 1H), 2.43 (dd, $J = 10$, 15, 1H), 2.72 (dd, $J = 6$, 15, 1H), 3.23 (dd, $J = 6$, 10, 1H), 3.33 (dd, $J = 6$, 10, 1H), 3.87 (s, 3H), 5.15 (s, 2H), 6.70–6.85 (m, 3H), 7.2–7.5 (m, 5H). Anal. ($\text{C}_{20}\text{H}_{25}\text{BrO}_2$) C, H, Br; calcd, 21.18; found, 20.74.

(2R,5S,2'S)-2-[2'-(3-Benzoyloxy-4-methoxy-benzyl)-3-methyl-butyl]-5-isopropyl-3,6-dimethoxy-2,5-dihydro-pyrazine (8). To a solution of (2*R*)-2-isopropyl-3,6-dimethoxy-2,5-dihydro-pyrazine (51.3 g, 0.273 mol) in THF (700 mL), cooled to -75°C , was added dropwise 1.6 M *n*-BuLi in hexane (170 mL, 0.273 mol) over 45 min. After 30 min at -75°C , a solution of **7** (68.7 g, 0.182 mol) in THF (0.3 L) was added dropwise over 30 min. The reaction mixture was stirred for 2 h at -75°C and overnight at -20°C . The mixture was concentrated, and the residue was partitioned between EtOAc (3×1 L) and water (3×1 L). The combined organics were washed with brine (1 L), dried (MgSO_4), and concentrated. FC purification (gradient CH_2Cl_2 /hexane 1:1 to 2:1 to 10:0) and repeated chromatography of enriched fractions afforded **8** (82.1 g, 94%) as a pale yellow oil: TLC $R_f = 0.22$ (CH_2Cl_2); $^1\text{H NMR}$ (300 MHz, CDCl_3) δ 0.68 (d, $J = 7$, 3H), 0.75 (m, 6H), 1.05 (d, $J = 7$, 3H), 1.2–1.85 (m, 4H), 2.27 (m, 1H), 2.35 (dd, $J = 10$, 15, 1H), 2.68 (dd, $J = 6$, 15, 1H), 3.66 (s, 6H), 3.86 (s, 3H), 3.97 (m, 2H), 5.12 (s, 2H), 6.7–6.85 (m, 3H), 7.25–7.45 (m, 5H); MS (EI) m/z 480 [M^+].

(2S,4S)-4-(3-Benzoyloxy-4-methoxy-benzyl)-2-tert-butoxycarbonylamino-5-methyl-hexanoic Acid Methyl Ester (9a). The solution of **8** (82.1 g, 0.171 mol) in MeCN (0.68 L) and 1 N HCl (0.68 L) was stirred at ambient temperature for 2 h. The mixture was poured into an ice-cold saturated aqueous solution of NaHCO_3 (2.5 L) and extracted with CH_2Cl_2 (3×1 L). The organic layers were washed with water (2×1 L), dried (Na_2SO_4), and evaporated.

FC purification (CH₂Cl₂/MeOH/NH₃ concd 100:5:0.1) yielded (2*S*,4*S*)-2-amino-4-(3-benzyloxy-4-methoxy-benzyl)-5-methyl-hexanoic acid methyl ester (55.5 g, 84%) as a pale yellow oil: TLC *R_f* = 0.38 (CH₂Cl₂/MeOH/NH₃ concd 700:10:10); HPLC *t_R* 14.8 min; ¹H NMR (300 MHz, CDCl₃) δ 0.80–0.85 (m, 6H), 1.2–1.8 (m, 6H), 2.43 (d, *J* = 7, 2H), 3.30 (m, 1H), 3.65 (s, 3H), 3.86 (s, 3H), 5.15 (s, 2H), 6.65–6.80 (m, 3H), 7.25–7.50 (m, 5H); MS (EI) *m/z* 385 [M]⁺.

To a solution of the above product (55.0 g, 0.143 mol) in CH₂Cl₂ (1.0 L), cooled to 0 °C, were subsequently added DIPEA (34.1 mL, 0.200 mol) and a solution of BOC₂O (40.4 g, 0.185 mol) in CH₂Cl₂ (200 mL). After warming to room temperature, the mixture was stirred overnight and then concentrated to give an oil that was FC purified (CH₂Cl₂/Et₂O 10:0 to 8:2). Compound **9a** (66.9 g, 97%) was obtained as pale yellow oil: TLC *R_f* = 0.66 (CH₂Cl₂/Et₂O 8:2); HPLC *t_R* 22.2 min; IR (CH₂Cl₂) 3433, 2956, 1588, 1437, 1367, 1026; ¹H NMR (300 MHz, CDCl₃) δ 0.7–0.8 (m, 6H), 1.35–1.65 (m, 13H), 2.35 (m, 1H), 2.62 (m, 1H), 3.70 (s, 3H), 3.86 (s, 3H), 4.35 (m, 1H), 4.84 (d, *J* = 8, 1H), 5.16 (s, 2H), 6.65–6.85 (m, 3H), 7.25–7.50 (m, 5H). Anal. (C₂₈H₃₉NO₆) C, H, N.

(1*S*,3*S*)-[1-Formyl-3-[4-methoxy-3-(3-methoxy-propoxy)-benzyl]-4-methyl-pentyl]-carbamic Acid *tert*-Butyl Ester (10b**).** The stirred solution of **9b**²⁶ (193 g, 0.40 mol) in toluene (2 L) was cooled to –70 °C, and a precooled 20% solution of DIBALH in toluene (800 mL, 0.96 mol) was added over 5 min at –75 to –80 °C (liquid ammonia cooling bath). Stirring at –75 °C was continued for 45 min, followed by addition of MeOH (80 mL) over 80 min while maintaining the temperature between –70° and –60 °C (**Caution**: vigorous gas evolution). The reaction mixture was poured with stirring into a mixture of 1 N HCl (4 L) and ice–water (2 kg), followed by addition of EtOAc (3 L). After 10 min, the organic layer was separated, and the aqueous phase was extracted twice with EtOAc (3 L). The combined organics were washed with water (2 × 4 L) and brine (1 × 4 L) and filtered over Hyflo. The filtrates were concentrated, taken up in toluene (1 L), concentrated, and dried in high vacuo at ambient temperature over 2 h to afford crude **10b** (190 g, ≥97%) as a pale yellow oil: TLC *R_f* = 0.44 (EtOAc/hexane 1:1); [α]_D²⁰ +14.6 ± 1.3 (*c* 0.78, CHCl₃); IR (CH₂Cl₂) 3431, 2959, 1710, 1589, 1514; ¹H NMR (CDCl₃) δ 0.86 (m, 6H), 1.44 (s, 9H), 1.55–1.8 (m, 4H), 2.09 (m, 2H), 2.4–2.7 (m, 2H), 3.35 (s, 3H), 3.57 (t, *J* = 7, 2H), 3.83 (s, 3H), 4.10 (t, *J* = 7, 2H), 4.05–4.4 (m, 1H), 4.89 (br d, *J* = 9, 1H), 6.8–6.8 (m, 3H), 9.50 (s, 1H).

(1*S*,2*S*,2'*S*)- and (1*S*,2*R*,2'*S*)-(4-Butylcarbamoyl-2-hydroxy-1-[2'-[4-methoxy-3-(3-methoxy-propoxy)-benzyl]-3'-methyl-butyl]-pent-4-enyl)-carbamic Acid *tert*-Butyl Ester (11b**) and (**12b**).** To a solution of *N*-butylmethacrylamide,²⁰ (see also Supporting Information; 82.8 g, 0.587 mol) in THF (1.3 L) was added a 1.6 M solution of *n*-BuLi in hexane (0.765 L, 1.22 mol) over 15 min at –78 °C. After warming to 0 °C for 30 min and recooling to –78 °C, the red-orange solution was subsequently treated with a 1 M solution of Ti(O^{*i*}-Pr)₃Cl in hexane (0.931 L, 0.931 mol) for 55 min and a solution of **10b** (126 g, 0.266 mol) in THF (0.7 L) for 15 min. Stirring of the dark colored solution for an additional 75 min at –78 °C was followed by quenching of the reaction by adding a saturated aqueous solution of NH₄Cl (1.6 L) at –20 °C. Then Et₂O (2 L) was added, and the mixture was stirred at 0–5 °C for 20 min. The organic layer was separated, and the aqueous phase was extracted with Et₂O (2 × 3 L). The combined organics were washed with water (2 × 4 L) and brine (3 L), dried (MgSO₄), and concentrated to provide the crude product as a mixture of the (2*S*)- and (2*R*)-configured diastereoisomers **11b/12b** in about a 2:3 ratio. Repeated FC purification on silica gel (EtOAc/hexane, gradient from 1:3 to 1:1) provided the pure isomers **11b** (76 g, 16.4%) and **12b** (188 g, 40%) as colorless oils.

Data for **11b**: TLC *R_f* = 0.21 (EtOAc/hexane 1:1); HPLC *t_R* 26.4 min (solvent gradient within 35 min); ¹H NMR (CDCl₃) δ 0.83 (m, 6H), 0.93 (t, *J* = 8, 3H), 1.05–1.8 (m, 8H), 1.43 (s, 9H), 2.09 (m, 2H), 2.28–2.51 (m, 3H), 2.65–2.75 (m, 1H), 3.30 (q, *J* = 8, 2H), 3.33 (s, 3H), 3.56 (t, *J* = 7, 2H), 3.5–3.7 (m, 2H), 3.82 (s, 3H), 4.10 (t, *J* = 7, 2H), 4.85 (d, *J* = 11, 1H), 5.10 (s, 1H),

5.40 (s, 1H), 5.56 (s, 1H), 6.08 (t, 1H), 6.65–6.85 (m, 3H). Anal. (C₃₂H₅₄N₂O₇) C, H, N.

Data for **12b**: TLC *R_f* = 0.16 (EtOAc/hexane 1:1); HPLC *t_R* 25.6 min (solvent gradient within 35 min); ¹H NMR (CDCl₃) δ 0.85 (d, *J* = 8, 6H), 0.93 (t, *J* = 8, 3H), 1.2–1.75 (m, 8H), 1.43 (s, 9H), 2.09 (m, 2H), 2.25–2.5 (m, 3H), 2.6–2.7 (m, 1H), 3.30 (q, *J* = 8, 2H), 3.33 (s, 3H), 3.56 (t, *J* = 7, 2H), 3.5–3.75 (m, 2H), 3.82 (s, 3H), 4.10 (t, *J* = 7, 2H), 4.75 (d, *J* = 11, 1H), 4.90 (s, 1H), 5.34 (s, 1H), 5.60 (s, 1H), 6.27 (t, 1H), 6.66–6.83 (m, 3H).

(1*S*,2*S*,4*R*,2'*S*)-(4-Butylcarbamoyl-2-hydroxy-1-[2'-[4-methoxy-3-(3-methoxy-propoxy)-benzyl]-3'-methyl-butyl]-pentyl)-carbamic Acid *tert*-Butyl Ester (13b**).** A solution of **11b** (81.0 g, 0.140 mol) in dry MeOH (800 mL) was hydrogenated at 25 bar pressure in the presence of Ru₂Cl₄[(*S*)-BINAP]₂NEt₃ (0.557 g) for 20 h at ambient temperature. Removal of solvent in vacuo gave the crude product as about a 9:1 mixture of the (4*R*)- and (4*S*)-diastereomers. Repeated recrystallization from Et₂O/hexane (0.45:1, 1.5 L) afforded the single isomer **13b** (57 g, 70%) as a white solid: mp 106.5–107 °C; TLC *R_f* = 0.19 (EtOAc/hexane 2:1); HPLC *t_R* 18.2 min; IR (CH₂Cl₂) 3437, 2959, 1703, 1667, 1588, 1513, 1465, 1391, 1367, 1234; ¹H NMR (DMSO-*d*₆; 80 °C) δ 0.79 (t, *J* = 8.0, 6H), 0.88 (t, *J* = 7.3, 3H), 1.02 (d, *J* = 6.9, 3H), 1.15–1.7 (m, 10H), 1.42 (s, 9H), 1.93 (m, 2H), 2.32 (m, 1H), 2.42 (m, 1H), 2.60 (m, 1H), 3.06 (m, 2H), 3.26 (s, 3H), 3.34 (m, 1H), 3.47 (m, 1H), 3.49 (t, *J* = 7, 2H), 3.70 (s, 3H), 4.00 (t, *J* = 7, 2H), 4.14 (d, *J* = 6.0, 1H), 5.72 (br s, 1H), 6.69 (dd, *J* = 2, 8, 1H), 6.78 (d, *J* = 2, 1H), 6.81 (d, *J* = 8, 1H), 7.23 (m, 1H). Anal. (C₃₂H₅₆N₂O₇) C, H, N.

(1*S*,2*S*,4*R*,2'*S*)-[4-Butylcarbamoyl-2-hydroxy-1-[2'-(3-hydroxy-4-methoxy-benzyl)-3-methyl-butyl]-pentyl]-carbamic Acid *tert*-Butyl Ester (14**).** A solution of **13a** (4.50 g, 7.51 mmol) in MeOH (60 mL) was hydrogenated in the presence of 5% palladium on charcoal (E 101N, Degussa; 0.9 g) for 60 min at ambient temperature. Removal of the catalyst over Celite and evaporation of the filtrates afforded **14** (3.78 g, quant.) as a colorless foam: mp 113–114 °C (Et₂O/hexane); TLC *R_f* = 0.21 (CH₂Cl₂/MeOH 9:1); HPLC *t_R* 18.0 min; FAB-MS *m/z* 509 [M + H]⁺; IR (CH₂Cl₂) 3535, 3436, 2960, 1666, 1591, 1456, 1366, 1239, 1170, 1029; ¹H NMR (500 MHz, DMSO-*d*₆, 70 °C) δ 0.75 (q, *J* = 7, 6, 6H), 0.86 (t, *J* = 7, 3H), 1.00 (d, *J* = 7, 3H), 1.1–1.7 (m, 10H), 1.39 (s, 9H), 2.20 (m, 1H), 2.45 (m, 1H), 2.55 (dd, *J* = 5, 15, 1H), 3.03 (q, *J* = 6, 13, 2H), 3.30 (m, 1H), 3.48 (m, 1H), 3.72 (s, 3H), 4.21 (d, *J* = 6, 1H), 5.88 (m, 1H), 6.53 (dd, *J* = 2, 8, 1H), 6.59 (d, *J* = 2, 1H), 6.75 (d, *J* = 8, 1H), 7.38 (m, 1H), 8.33 (br s, 1H). Anal. (C₂₈H₄₈N₂O₆) C, H, N.

(1*S*,3*S*,2'*S*,4'*R*)-[4-Methoxy-3-(3-methoxy-propoxy)-benzyl]-4-methyl-1-(4'-methyl-5-oxo-tetrahydro-furan-2'-yl)-pentyl]-carbamic Acid *tert*-Butyl Ester (15**).** The mixture of **13b** (5.64 g, 9.64 mmol) and *p*-TsOH·H₂O (2.02 g, 10.6 mmol) in CHCl₃ (240 mL) was kept for 18 h at ambient temperature, followed by evaporation to a small volume. Et₂O was added, and the organic layer was washed with 0.1 M HCl and brine, dried (MgSO₄), and evaporated. FC purification (EtOAc/hexane 1:1) and recrystallization from Et₂O/hexane yielded **15** (3.67 g, 75%); mp 86–88 °C; TLC *R_f* = 0.47 (EtOAc/hexane 2:1); HPLC *t_R* 17.2 min; ¹H NMR (CDCl₃) δ 0.82 (d, *J* = 8, 6H), 1.26 (d, *J* = 8, 3H), 1.45 (s, 9H), 1.4–1.75 (m, 4H), 1.90 (m, 1H), 2.10 (t, *J* = 6, 2H), 2.3–2.45 (m, 2H), 2.6–2.75 (m, 2H), 3.35 (s, 3H), 3.56 (t, *J* = 7, 2H), 3.75–3.9 (m, 1H), 3.83 (s, 3H), 4.10 (t, *J* = 7, 2H), 4.37 (d, *J* = 2, 1H), 4.45 (m, 1H), 6.67 (dd, *J* = 2, 8, 1H), 6.72 (d, *J* = 2, 1H), 6.78 (d, *J* = 8, 1H); MS(FAB) *m/z* 507 [M + H]⁺. Anal. (C₂₈H₄₅NO₇) C, H, N.

(2*R*,4*S*,5*S*,7*S*)-5-*tert*-Butoxycarbonylamino-4-(*tert*-butyl-dimethyl-silyloxy)-7-[4-methoxy-3-(3-methoxy-propoxy)-benzyl]-2,8-dimethyl-nonanoic Acid (17**).** To a solution of **15** (3.60 g, 7.12 mmol) in 1,2-DME/H₂O (2:1; 210 mL) was added 1 M LiOH (28.5 mL, 28.5 mmol). After 1 h at room temperature, volatiles were removed in vacuo, followed by addition of an ice-cold 10% aqueous solution of citric acid (60 mL). Extraction of the water phase with CHCl₃ (4 × 150 mL), drying of the combined organics

(MgSO₄), and evaporation of solvents gave the crude product **16**, which was used directly in the next reaction step.

To a solution of the above material in dry DMF (45 mL) was added TBDMSiCl (2.36 g, 15.66 mmol) and imidazole (2.03 g, 29.9 mmol), and the mixture was kept for six days at room temperature. The solvent was removed under reduced pressure, and the residue was partitioned between EtOAc and a 10% aqueous solution of citric acid. The layers were separated, and the organic phase was washed with water and brine and dried (MgSO₄). After evaporation of the solvent, the residue (TLC *R_f* = 0.82; EtOAc/hexane 1:1) was dissolved in THF (20 mL), water (8 mL) and acetic acid (20 mL), and the mixture was stirred at ambient temperature overnight. After removal of the solvent, ice/water was added to the residue, followed by extraction with EtOAc (3 × 250 mL). The combined organics were washed with water and brine, dried (MgSO₄), and evaporated. FC purification (EtOAc/hexane (1:1) gave **17** (3.11 g, 68%) as a colorless oil: TLC *R_f* = 0.25 (EtOAc/hexane 1:1); HPLC *t_R* 24.0 min; ¹H NMR (DMSO-*d*₆; 80 °C) δ 0.08 (s, 6H), 0.80 (m, 6H), 0.88 (s, 9H), 1.09 (d, *J* = 7, 3H), 1.25 (m, 2H), 1.40 (m, 1H), 1.42 (s, 9H), 1.55–1.7 (m, 2H), 1.88 (m, 1H), 1.92 (m, 2H), 2.31 (m, 1H), 2.45 (m, 1H), 2.57 (m, 1H), 3.26 (s, 3H), 3.49 (t, *J* = 7, 2H), 3.61 (m, 1H), 3.70 (m, 1H), 3.74 (s, 3H), 4.00 (t, *J* = 7, 2H), 5.76 (br s, 1H), 6.68 (d, *J* = 8, 1H), 6.76 (s, 1H), 6.82 (d, *J* = 8, 1H); FAB-MS *m/z* 640 [M + H]⁺. Anal. (C₃₄H₆₁NO₈Si) C, H, N.

General Procedures. A. O-Alkylation of Intermediate 14 (Scheme 3). The general procedure is exemplified by the synthesis of compound **18**: To a suspension of NaH (60–65% in mineral oil; 14 mg, 0.324 mmol) in DMF (2 mL) was added dropwise a solution of **14** (0.150 g, 0.295 mmol) in DMF (1 mL) at ambient temperature. After 30 min, a solution of *n*-pentyl iodide (117 mg, 0.590 mmol) in DMF (1 mL) was added and stirring was continued for 16 h. Solvents were evaporated, the residue was dissolved in H₂O (15 mL) followed by extraction of the aqueous layer with Et₂O (2 × 20 mL). The organics were dried (MgSO₄) and evaporated, and the residue was purified by flash chromatography (CH₂Cl₂/Et₂O 2:1). Recrystallization from Et₂O/hexane afforded **18** (0.120 g, 70%) as a white solid: mp 104–105 °C; TLC *R_f* = 0.21 (CH₂Cl₂/MeOH 9:1); HPLC *t_R* 23.7 min; IR (CH₂Cl₂) 3437, 2960, 2934, 1703, 1514, 1236, 1164; ¹H NMR (DMSO-*d*₆) δ 0.71 (m, 6H), 0.86 (m, 6H), 0.97 (d, *J* = 7, 3H), 1.0–1.7 (m, 16H), 1.34 (s, 9H), 2.20 (dd, *J* = 10, 15, 1H), 2.43 (m, 1H), 2.61 (dd, *J* = 5, 15, 1H), 3.01 (m, 2H), 3.25 (m, 1H), 3.49 (m, 1H), 3.69 (s, 3H), 3.88 (m, 2H), 4.38 (d, *J* = 7, 1H), 6.17 (d, *J* = 10, 1H), 6.63 (dd, *J* = 2, 10, 1H), 6.76 (d, *J* = 2, 1H), 6.78 (d, *J* = 10, 1H), 7.60 (m, 1H). Anal. (C₃₃H₅₈N₂O₆) C, H, N.

Compound 13b (Method B). Compound **13b** obtained as described above from **14** (1.2 g, 2.36 mmol), NaH (60–65% in mineral oil; 103 mg, 2.59 mmol) and 3-methoxypropyl iodide (0.63 g, 3.16 mmol) in DMF (80 mL) followed by FC purification on silica gel (CH₂Cl₂/MeOH 95:5) afforded the product as a white foam (1.18 g, 86%): TLC *R_f* = 0.52 (CH₂Cl₂/MeOH 95:5); FAB-MS *m/z* 582 [M + H]⁺.

The *N*-Boc derivatives of compounds **28**, **29**, **34** (Table 1), and **36–42** (Table 2) were obtained in a similar manner by using the corresponding alkyl halides. The *N*-Boc derivative **30** was obtained by the reaction of *N*-Boc-**28** (28.8 mg, 0.05 mmol) with methylamine (1 mL) in DMF (3 mL) in a sealed tube for 60 h at room temperature to give, after FC purification (CH₂Cl₂/MeOH 9:1), a colorless oil (18.6 mg, 62%).

B. N-Boc-Deprotection. The renin inhibitors listed in Tables 1–5 were obtained, if not otherwise stated, as their hydrochloride salts by final *N*-Boc-deprotection under standard reaction conditions as described for the following examples:

(2R,4S,5S,7S)-5-Amino-4-hydroxy-7-(4-methoxy-3-pentyloxy-benzyl)-2,8-dimethyl-nonanoic Acid Butylamide, Hydrochloride Salt (43·HCl). A solution of **18** (53 mg, 0.092 mmol) in 4 N HCl/dioxane (1 mL) was rigorously stirred for 2 h at 0 °C. Subsequent freeze-drying in high vacuo gave **43·HCl** (47 mg) as an amorphous solid: TLC *R_f* = 0.22 (CH₂Cl₂/MeOH 9:1); HPLC *t_R* 16.7 min; ¹H NMR (DMSO-*d*₆) δ 0.80 (m, 6H), 0.86 (m, 6H), 1.01 (d, *J* = 7,

3H), 1.15–1.5 (m, 11H), 1.55 (m, 1H), 1.65–1.75 (m, 3H), 1.80 (m, 1H), 2.35–2.5 (m, 2H), 2.55 (m, 1H), 2.70 (m, 1H), 3.03 (m, 2H), 3.30 (m, 1H), 3.70 (s, 3H), 3.92 (t, *J* = 7, 2H), 5.47 (br s, 1H), 6.70 (dd, *J* = 2, 10, 1H), 6.8–6.85 (m, 2H), 7.66 (br s, 3H), 7.92 (m, 1H); HRMS *m/z* 479.3883 [(M + H)⁺ calcd for C₂₈H₅₀N₂O₄⁺, 479.3849].

Compound 38a·HCl. Compound **38a·HCl** was obtained as described above by dissolving **13b** (1.13 g, 1.94 mmol; obtained by method B) in 4 N HCl/dioxane (40 mL), cooled to 0 °C, followed by reaction at room temperature for 30 min and subsequent freeze-drying in high vacuo to afford the product (0.99 g, 99%) as a pale beige foam: TLC *R_f* = 0.13 (CH₂Cl₂/MeOH 9:1); HPLC *t_R* 23.7 min (97.0% purity); HRMS *m/z* 481.3641 [(M + H)⁺ calcd for C₂₇H₄₈N₂O₅⁺, 481.3615].

C. Direct Aminolysis of Lactone 15 (Scheme 3). (1S,2S,4R,2'S)-(2-Hydroxy-4-(3-hydroxy-propylcarbamoyl)-1-{2'-[4-methoxy-3-(3-methoxy-propoxy)-benzyl]-3-methyl-butyl}-pentyl)-carbamoyl tert-Butyl Ester (20). Lactone **15** (0.102 g, 0.20 mmol) and neat 3-amino-1-propanol (0.50 mL, 6.57 mmol) were heated at 80 °C for 1 h. To the reaction mixture was added ice-cold 1 N HCl (30 mL), followed by extraction of the water phase with EtOAc (2 × 25 mL). The combined organics were washed with H₂O (1 × 30 mL) and a saturated solution of NaHCO₃ (1 × 20 mL) and dried (MgSO₄). FC purification (CH₂Cl₂/MeOH 9:1) and recrystallization from Et₂O yielded **20** (0.095 g, 82%) as a white solid: mp 100–101 °C; TLC *R_f* = 0.43 (CH₂Cl₂/MeOH 9:1); HPLC *t_R* 16.5 min; IR (CH₂Cl₂) 3436, 2959, 2935, 1702, 1654, 1514, 1237, 1163; ¹H NMR (DMSO-*d*₆) δ 0.73 (t, *J* = 7, 6H), 0.95–1.5 (m, 7H), 0.98 (d, *J* = 7, 3H), 1.37 (s, 9H), 1.90 (m, 2H), 2.21 (m, 1H), 2.4–2.55 (m, 3H), 2.63 (m, 1H), 3.07 (m, 2H), 3.26 (s, 3H), 3.38 (m, 2H), 3.44 (m, *J* = 7, 2H), 3.48 (m, 1H), 3.70 (s, 3H), 3.94 (m, 2H), 4.38 (m, 2H), 6.17 (d, *J* = 10, 1H), 6.64 (dd, *J* = 2, 8, 1H), 6.76 (d, *J* = 2, 1H), 6.78 (d, *J* = 8, 1H), 7.64 (t, *J* = 6, 1H). Anal. (C₃₁H₅₄N₂O₈) C, H, N.

Inhibitors **44–46**, **48–57**, **60**, **63**, and **70–74** (Tables 3–5) were synthesized in a similar manner as described above.

D. Coupling to Acid 17 and Removal of the O-TBDMSI Protecting Group (Scheme 4). (2R,4S,5S,7S)-3-{5-tert-Butoxycarbonylamino-4-(tert-butyl-dimethyl-silyloxy)-7-[4-methoxy-3-(3-methoxy-propoxy)-benzyl]-2,8-dimethyl-nonanoylamino}-propionic Acid Ethyl Ester (21). To a solution of **17** (0.160 g, 0.25 mmol) in DMF (10 mL) at 0 °C was added subsequently Et₃N (0.084 mL, 0.60 mmol), β-alanine ethylester HCl (0.046 g, 0.30 mmol), and diethyl cyanophosphonate (0.048 mL, 0.30 mmol). After stirring for 20 h at room temperature, the mixture was concentrated and a 10% aqueous solution of citric acid (20 mL) was added. Extraction with EtOAc (2 × 20 mL) was followed by washing of the organics with a saturated NaHCO₃ (20 mL) and brine (20 mL). FC purification (EtOAc/hexane 1:1) afforded **21** (0.174 g, 94%) as a colorless oil: TLC *R_f* = 0.28 (EtOAc/hexane 1:1); HPLC *t_R* 27.2 min; ¹H NMR (DMSO-*d*₆) δ 0.02 (s, 3H), 0.05 (s, 3H), 0.74 (t, *J* = 7, 6H), 0.85 (s, 9H), 0.99 (d, *J* = 7, 3H), 1.05–1.6 (m, 5H), 1.18 (t, *J* = 7, 3H), 1.42 (s, 9H), 1.8–2.65 (m, 5H), 1.90 (m, 2H), 3.2–3.65 (m, 5H), 3.26 (s, 3H), 3.44 (t, *J* = 7, 2H), 3.69 (s, 3H), 3.93 (t, *J* = 7, 2H), 4.04 (m, 2H), 6.31 (d, *J* = 10, 1H), 6.63 (dd, *J* = 2, 8, 1H), 6.71 (d, *J* = 2, 1H), 6.78 (d, *J* = 8, 1H), 7.64 (t, *J* = 6, 1H). Anal. (C₃₉H₇₀N₂O₉Si) C, H, N.

(2R,4S,5S,7S)-3-{5-tert-Butoxycarbonylamino-4-hydroxy-7-[4-methoxy-3-(3-methoxy-propoxy)-benzyl]-2,8-dimethyl-nonanoylamino}-propionic Acid Ethyl Ester (22). A solution of **21** (0.155 g, 0.210 mmol) and tetrabutyl-ammonium-fluoride trihydrate (0.132 g, 0.420 mmol) in DMF (10 mL) was stirred for 2 h at ambient temperature. The mixture was concentrated, and the residue was partitioned between EtOAc (2 × 30 mL) and water–brine (1:1, 30 mL). The usual workup and FC purification (EtOAc/hexane 2:1) gave **22** (0.105 g, 80%) as a colorless oil: mp 85–86 °C (recrystallized from Et₂O/hexane); TLC *R_f* = 0.12 (EtOAc/hexane 2:1); HPLC *t_R* 17.5 min; ¹H NMR (CDCl₃) δ 0.83 (m, 6H), 1.05–1.75 (m, 6H), 1.15 (d, *J* = 7, 3H), 1.27 (t, *J* = 7, 3H), 1.45 (s, 9H), 2.08 (m, 2H), 2.35–2.65 (m, 5H), 3.35 (s, 3H), 3.4–3.6 (m, 5H), 3.57 (t, *J* = 7, 2H), 3.82 (s, 3H), 4.10 (t, *J* = 7, 2H), 4.15 (m,

2H), 4.67 (d, $J = 12$, 1H), 6.32 (br m, 1H), 6.70 (dd, $J = 2$, 8, 1H), 6.77 (d, $J = 8$, 1H), 6.78 (m, 1H). Anal. (C₃₃H₅₆N₂O₉) C, H, N.

(2R,4S,5S,7S)-3-[5-*tert*-Butoxycarbonylamino-4-hydroxy-7-[4-methoxy-3-(3-methoxy-propoxy)-benzyl]-2,8-dimethyl-nonanoylamino]-propionic Acid (23). To a solution of **22** (70 mg, 0.112 mmol) in MeOH (2 mL) was added 1 N NaOH (0.224 mL, 0.224 mmol). After 18 h at ambient temperature, the volatiles were removed under reduced pressure. The residue was taken up in water (15 mL) and the aqueous phase was acidified by adding 1 N HCl (0.25 mL). Extractive workup with EtOAc (2 × 15 mL) and FC purification (CH₂Cl₂/MeOH 8:2) afforded **23** (60 mg, 90%) as a white amorphous solid: TLC $R_f = 0.12$ (CH₂Cl₂/MeOH 9:1); HPLC t_R 16.8 min; ¹H NMR (DMSO-*d*₆) δ 0.74 (t, $J = 7$, 6H), 0.97 (d, $J = 7$, 3H), 1.0–1.65 (m, 5H), 1.39 (s, 9H), 1.95 (m, 2H), 2.1–2.25 (m, 3H), 2.43 (m, 1H), 2.64 (m, 1H), 3.15–3.55 (m, 6H), 3.23 (s, 3H), 3.30 (s, 1H, COOH + H₂O), 3.44 (t, $J = 7$, 2H), 3.70 (s, 3H), 3.94 (t, $J = 7$, 2H), 6.16 (d, $J = 10$, 1H), 6.65 (dd, $J = 2$, 8, 1H), 6.75 (d, $J = 2$, 1H), 6.78 (d, $J = 8$, 1H), 7.64 (br m, 1H).

Inhibitors **47–48**, **58–62**, **64–69**, and **75–77** (Tables 3–5) were synthesized in a similar manner as described above.

Large-Scale Preparation of Inhibitor **38a**, Hydrochloride Salt.

To a solution of **13b** (57 g, 0.098 mol) in EtOAc (300 mL) was added 4 N HCl in EtOAc (600 mL) at -5 °C. The mixture was stirred for 18 h at $0-2$ °C, followed by removal of the solvent under reduced pressure at room temperature. The residue was dried in high vacuo at 35 °C over 48 h to yield the title compound (50.8 g) as a white amorphous powder: mp $60-70$ °C; TLC $R_f = 0.24$ (CH₂Cl₂/MeOH 9:1); HPLC t_R 11.8 min; $[\alpha]_D^{20} -29.4 \pm 0.8$ (c 1.2, CHCl₃); IR (CH₂Cl₂) 2959, 1661, 1515, 1465, 1388, 1235; ¹H NMR (DMSO-*d*₆) δ 0.81 (t, $J = 7$, 6H), 0.86 (t, $J = 7$, 3H), 1.00 (d, $J = 7$, 3H), 1.1–1.9 (m, 9H), 1.93 (m, 2H), 2.35–2.6 (m, 3H), 2.73 (m, 1H), 3.04 (m, 2H), 3.25 (s, 3H), 3.30 (m, 1H), 3.47 (t, $J = 7$, 2H), 3.72 (s, 3H), 3.98 (t, $J = 7$, 2H), 5.48 (br s, 1H), 6.71 (dd, $J = 2$, 8, 1H), 6.82 (s, 1H), 6.84 (d, $J = 2$, 1H), 7.69 (br s, 3H, NH₃⁺), 7.92 (t, $J = 6$, 1H). Anal. (C₂₇H₄₉ClN₂O₅·0.16H₂O) C, H, N; Cl: calcd, 6.82; found, 7.28.

Biological Materials and Methods. In vitro enzyme inhibition by newly synthesized compounds was determined as described previously.⁹ In brief, human recombinant renin (0.33 ng/mL) was incubated with a synthetic tetradecapeptide substrate (TDP, 13.33 μ M) corresponding to the 14 amino terminal amino acids of human angiotensinogen, in 0.33 M TES buffer, pH 7.2, containing 1% (w/v) human serum albumin (HSA) and 0.1% neomycin sulfate, for 1 h at 37 °C. Total volume of the incubation solution was 60 μ L. The enzymatic reaction was stopped by adding 1 mL of ice-cold 0.1 M Tris-acetate buffer, pH 7.4, containing 0.1% HSA. The Ang I generated during the incubation was measured by radioimmunoassay.⁵³

Human and Marmoset Plasma Renin Assay. Determining the IC₅₀ for Inhibition of Endogenous Renin in Plasma from Human and Marmosets. Plasma collected on EDTA was incubated with the angiotensinase inhibitor, 2,3-dimercaptoethanol (5 mM) at pH 7.2 (0.5 M Tris [hydroxymethyl]aminomethane acetate buffer), in the absence or presence of inhibitor (0.1 nM–10 μ M) for 1 h at 37 °C. The Ang I generated was quantified by radioimmunoassay.⁵³

Blood Pressure and Heart Rate Measurements in Marmosets. Systolic and diastolic BP, as well as heart rate, were measured by telemetry in conscious, freely moving marmosets (250–350 g in weight), as described previously.⁴⁶ Pressure transmitters (AM Unit, model TA11PA-C40, Data Sciences Inc., St. Paul, Minnesota) were implanted into the peritoneal cavity under aseptic conditions and light anaesthesia, and the sensor catheter was placed in the aorta below the renal artery pointing upstream.⁴⁶ Marmosets were allowed to recover for at least four weeks before any experiment. Marmosets were maintained on a low sodium diet (pellets with Na⁺, 9 mmol/kg, and K⁺, 128 mmol/kg, NAFAG, Gossau, Switzerland), supplemented with fruit, and with free access to water for 1 week before and during experiments.

Determination of PRA in Marmosets. Plasma renin activity (PRA) was measured at different time points (1.5, 3, 6, and 24 h

after administration of the inhibitor) by the antibody trapping method⁴⁸ from blood samples collected by direct puncture of a femoral vein using EDTA as an anticoagulant. For each animal, percentage inhibition of PRA at each time point was calculated using the pretreatment PRA as the baseline.

Acknowledgment. We are grateful to Dr. Eric Francotte and Mr. Paul Richert for analytical chiral HPLC separations. The authors thank Dr. Nils Ostermann for providing the illustrations in Figures 3 and 4 and for critical discussions. Richard Göschke is indebted to Ms. Nicole Hasler and Ms. Florence Kummlig-Lugrin for their excellent technical assistance. Technical and editorial assistance was provided by Geoff Davison (ACUMED, Macclesfield, U.K.).

Supporting Information Available: Additional data on analytical characterization of the final inhibitor compounds, experimental procedures for the preparation of *N*-butyl-2-methyl-acrylamide, compounds **10a**, **11a**, **12a**, **13a**, **24–26**, **44**, **48**, **58**, and **60**, as well as for P2' amines used in the synthesis of inhibitors **57**, **67**, **71–73**, and **77**, and X-ray crystallographic data for compound **13b**. This material is available free of charge via the Internet at <http://pubs.acs.org>.

References

- (1) World Health Organization, International Society of Hypertension Group. 2003 World Health Organization (WHO)/International Society of Hypertension (ISH) Statement on Management of Hypertension. *J. Hypertens.* **2003**, *21*, 1983–1992.
- (2) American Heart Association, Statistics, 2004.
- (3) Hackenthal, E.; Paul, M.; Ganten, D.; et al. Morphology, Physiology, and Molecular Biology of Renin Secretion. *Physiol. Rev.* **1990**, *70*, 1067–1116.
- (4) Brewster, U. C.; Perazella, M. A. The Renin-Angiotensin-Aldosterone System and the Kidney: Effects on Kidney Disease. *Am. J. Med.* **2004**, *116*, 263–272.
- (5) Hershey, J. C.; Steiner, B.; Fischli, W.; Feuerstein, G. Renin Inhibitors: An Antihypertensive Strategy on the Verge of Reality. *Drug Discovery Today: Therapeutic Strategies* **2005**, *2*, 181–185.
- (6) Wier, M. R.; Dzau, V. J. The Renin-Angiotensin-Aldosterone System: A Specific Target for Hypertension Management. *Am. J. Hypertens.* **1999**, *12*, 205S–213S.
- (7) Weber, M. A. Interrupting the Renin-Angiotensin System: The Role of Angiotensin-Converting Enzyme Inhibitors and Angiotensin II Receptor Antagonists in the Treatment of Hypertension. *Am. J. Hypertens.* **1999**, *12*, 189S–194S.
- (8) Fisher, N. D. L.; Hollenberg, N. K. Renin Inhibition: What are the Therapeutic Opportunities? *J. Am. Soc. Nephrol.* **2005**, *16*, 592–599.
- (9) Wood, J. M.; Gulati, N.; Forgiarini, P.; Fuhrer, W.; Hofbauer, K. G. Effects of a Specific and Long-Acting Renin Inhibitor in the Marmoset. *Hypertension* **1985**, *7*, 797–803.
- (10) Azizi, M.; Guyene, T. T.; Chatellier, G.; Menard, J. Blood Pressure Effects of Acute Intravenous Renin or Oral Angiotensin Converting Enzyme Inhibition in Essential hypertension. *J. Hypertens.* **1994**, *12*, 419–427.
- (11) Glassman, H. N.; Kleinert, H. D.; Boger, R. S.; Moyses, D. M.; Griffiths, A. N.; Luther, R. R. Clinical Pharmacology of Enalkiren, a Novel, Dipeptide Renin Inhibitor. *J. Cardiovasc. Pharmacol.* **1990**, *16* (Suppl. 4), S76–S81.
- (12) Neutel, J. M.; Luther, R. R.; Boger, R. S.; Weber, M. A. Immediate Blood Pressure Effects of the Renin Inhibitor Enalkiren and the Angiotensin-Converting Enzyme Inhibitor Enalaprilat. *Am. Heart J.* **1991**, *122*, 1094–1100.
- (13) Greenlee, W. J. Renin Inhibitors. *Med. Res. Rev.* **1990**, *10*, 173–236.
- (14) Ocain, T. D.; Abou-Gharbia, M. Renin-Angiotensin System (RAS) Dependent Antihypertensive Agents: Renin Inhibitors. *Drugs Future* **1991**, *16*, 37–51.
- (15) Kleinert, H. Recent Developments in Renin Inhibitors. *Expert Opin. Invest. Drugs* **1994**, *3*, 1087–104.
- (16) Rosenberg, S. H. Renin Inhibitors. In *Progress in Medicinal Chemistry*; Ellis, G. P., Luscombe, D. K., Eds.; Elsevier Science: New York, 1995; Vol. 32, pp 37–115.
- (17) Rosenberg, S. H.; Kleinert, H. D. Renin Inhibitors. *Pharm. Biotech.* **1998**, *11*, 7–28.

- (18) Bühlmayer, P.; Caselli, A.; Fuhrer, W.; Göschke, R.; Rasetti, V.; Rueger, H.; Stanton, J. L.; Criscione, L.; Wood, J. L. Synthesis and Biological Activity of Some Transition-State Inhibitors of Human Renin. *J. Med. Chem.* **1988**, *31*, 1839–1846.
- (19) Rasetti, V.; Cohen, N. C.; Rueger, H.; Göschke, R.; Maibaum, J.; Cumin, F.; Fuhrer, W.; Wood, J. M. Bioactive Hydroxyethylene Dipeptide Isosteres with Hydrophobic (P3–P1)-Moieties. A Novel Strategy Towards Small Non-Peptide Renin Inhibitors. *Bioorg. Med. Chem. Lett.* **1996**, *6*, 1589–1594.
- (20) Göschke, R.; Cohen, N. C.; Wood, J. M.; Maibaum, J. Design and Synthesis of Novel 2,7-Dialkyl Substituted 5(S)-Amino-4(S)-hydroxy-8-phenyl-octanecarboxamides as In Vitro Potent Peptidomimetic Inhibitors of Human Renin. *Bioorg. Med. Chem. Lett.* **1997**, *7*, 2735–2740.
- (21) Maibaum, J.; Rasetti, V.; Rueger, H.; Cohen, N. C.; Göschke, R.; Mah, R.; Rahuel, J.; Gruetter, M. G.; Cumin, F.; Wood, J. M. Design and Synthesis of Novel Potent, Non-Peptide and Orally Active Renin Inhibitors. In *Medicinal Chemistry: Today and Tomorrow*, Proceedings of the AFMC International Medicinal Chemistry Symposium, Tokyo, September 3–8, 1995; Yamazaki, M., Ed.; Blackwell Science: U.K., 1997; pp 155–162.
- (22) Rahuel, J.; Rasetti, V.; Maibaum, J.; Rueger, H.; Göschke, R.; Cohen, N. C.; Stutz, S.; Cumin, F.; Fuhrer, W.; Wood, J. M.; Gruetter, M. G. Structure-Based Drug Design: The Discovery of Novel Nonpeptide Orally Active Inhibitors of Human Renin. *Chem. Biol.* **2000**, *7*, 493–504.
- (23) Maibaum, J.; Cohen, N.-C.; Rahuel, J.; Gruetter, M. G.; Schnell, Ch.; Baum, H.-P.; Rigollier, P.; Schilling, W.; Wood, J. M. Design and Synthesis of Novel, Fully Nonpeptide Transition State Mimetic Renin Inhibitors Bearing an *O*-Alkyl Substituted Salicylamide (P3^{sp}-P3)-Moieties with High Oral in vivo Potency. Proceedings of the XVth EFMC International Symposium on Medicinal Chemistry, Edinburgh, U.K., September 6–10, 1998; Abstract Book P231.
- (24) Göschke, R.; Rasetti, R.; Cohen, N.-C.; Rahuel, J.; Gruetter, M. G.; Stutz, S.; Rueger, H.; Fuhrer, W.; Wood, J. M.; Maibaum, J. Novel 2,7-Dialkyl Substituted 5(S)-Amino-4(S)-hydroxy-8-phenyl-octanecarboxamide Transition State Peptidomimetics are Potent and Orally Active Inhibitors of Human Renin. Proceedings of the XVth EFMC International Symposium on Medicinal Chemistry, Edinburgh, U.K., September 6–10, 1998; Abstract Book P229.
- (25) Schöllkopf, U.; Groth, U.; Deng, C. Asymmetric Syntheses via Heterocyclic Intermediates. 4. Enantioselective Synthesis of (*R*)-Amino Acids by use of L-Valine as Chiral Auxiliary Agent. *Angew. Chem.* **1981**, *93*, 793–795.
- (26) Göschke, R.; Stutz, S.; Heinzlmann, W.; Maibaum, J. The Nonchiral Bislactim Diethoxy Ether as a Highly Stereo-Inducing Synthon for Sterically Hindered, γ -Branched α -Amino Acids: A Practical, Large-Scale Route to an Intermediate of the Novel Renin Inhibitor Aliskiren. *Helv. Chim. Acta* **2003**, *86*, 2848–2870.
- (27) Kempf, D. J. Dipeptide Analogs. Versatile Synthesis of the Hydroxyethylene Isostere. *J. Org. Chem.* **1986**, *51*, 3921–3926.
- (28) Ohta, T.; Takaya, H.; Kitamura, M.; Nagai, K.; Noyori, R. Asymmetric Hydrogenation of Unsaturated Carboxylic Acids Catalyzed by BINAP-Ruthenium(II) Complexes. *J. Org. Chem.* **1987**, *52*, 3174–3176.
- (29) Evans, B. E.; Rittle, K. E.; Homnick, C. F.; Springer, J. P.; Hirshfield, J.; Veber, D. F. A Stereocontrolled Synthesis of Hydroxyethylene Dipeptide Isosteres Using Novel, Chiral Aminoalkyl Epoxides and γ -(Aminoalkyl) γ -Lactones. *J. Org. Chem.* **1985**, *50*, 4615–4625.
- (30) Spek, A. L. Single-Crystal Structure Validation with the Program PLATON. *J. Appl. Cryst.* **2003**, *36*, 7–13.
- (31) Flack, H. D. On Enantiomorph-Polarity Estimation. *Acta Crystallogr.* **1983**, *A39*, 876–881.
- (32) Evans, B. E.; Rittle, K. E.; Bock, M. G.; Bennett, C. D.; DiPardo, R. M.; Boger, J.; Poe, M.; Ulm, E. H.; LaMont, B. I.; Blaine, E. H.; Fanelli, G. M.; Stabilito, I. I.; Veber, D. F.; A Uniquely Potent Renin Inhibitor and Its Unanticipated Plasma Binding Component. *J. Med. Chem.* **1985**, *28*, 1755–1756.
- (33) Märki, H. P.; Binggeli, A.; Bittner, B.; Bohner-Lang, V.; Brey, V.; Bur, D.; Coassolo, Ph.; Clozel, J. P.; D'Arcy, A.; Doebeli, H.; Fischli, W.; Funk, Ch.; Foricher, J.; Giller, T.; Grüninger, F.; Guenzi, A.; Güller, R.; Hartung, T.; Hirth, G.; Jenny, Ch.; Kansy, M.; Klinkhammer, U.; Lave, T.; Lohri, B.; Luft, F. C.; Mervaala, E. M.; Müller, D. N.; Müller, M.; Montavon, F.; Oefner, Ch.; Qiu, C.; Reichel, A.; Sanwald-Ducray, P.; Scalone, M.; Schleimer, M.; Schmid, R.; Stadler, H.; Treiber, A.; Valdenaire, O.; Vieira, E.; Waldmeier, P.; Wiegand-Chou, R.; Wilhelm, M.; Wostl, W.; Zell, M.; Zell, R. Piperidine Renin Inhibitors: From Leads to Drug Candidates. *Il Farmaco* **2001**, *56*, 21–27.
- (34) Vieira, E.; Binggeli, A.; Brey, V.; Bur, D.; Fischli, W.; Güller, R.; Hirth, G.; Märki, H. P.; Müller, M.; Oefner, C.; Scalone, M.; Stadler, H.; Wilhelm, M.; Wostl, W. Substituted Piperidines—Highly Potent Renin Inhibitors Due To Induced Fit Adaptation of the Active Site. *Bioorg. Med. Chem. Lett.* **1999**, *9*, 1397–1402.
- (35) Boyd, S. A.; Fung, A. K. L.; Baker, W. R.; Mantei, R. A.; Stein, H. H.; Cohen, J.; Barlow, J. L.; Klinghofer, V.; Wessale, J. L.; et al. Nonpeptide Renin Inhibitors with Good Intraduodenal Bioavailability and Efficacy in Dog. *J. Med. Chem.* **1994**, *37*, 2991–3007.
- (36) Boyd, S. A.; Fung, A. K. L.; Baker, W. R.; Mantei, R. A.; Armiger, Yoek, L.; Stein, H. H.; Cohen, J.; Egan, D. A.; Barlow, J. L.; et al. C-Terminal Modifications of Nonpeptide Renin Inhibitors: Improved Oral Bioavailability via Modification of Physicochemical Properties. *J. Med. Chem.* **1992**, *35*, 1735–1746.
- (37) DeLano, W. L. The PyMOL Molecular Graphics System. DeLano Scientific LLC, San Carlos, CA, U.S.A., 2002; <http://www.pymol.org>
- (38) Rahuel, J.; Priestle, J. P.; Gruetter, M. G. The Crystal Structures of Recombinant Glycosylated Human Renin Alone and in Complex with a Transition-State Analog Inhibitor. *J. Struct. Biol.* **1991**, *107*, 227–236.
- (39) Chen, Y. W.; Fersht, A. R.; Henrick, K. Contribution of Buried Hydrogen Bonds to Protein Stability. *J. Mol. Biol.* **1993**, *234*, 1158–1170.
- (40) Hanson, G. J.; Clare, M.; Summers, N. L.; Lim, L. W.; Neidhart, D. J.; Shieh, H. S.; Stevens, A. M. Renin Inhibitor SC-51106 Complexed with Human Renin: Discovery of a New Binding Site Adjacent to P3. *Bioorg. Med. Chem.* **1994**, *2*, 909–918.
- (41) Tong, L.; Pav, S.; Lamarre, D.; Pilote, L.; LaPlante, S.; Anderson, P. C.; Jung, G. High Resolution Crystal Structures of Recombinant Human Renin in Complex with Polyhydroxymonoamide Inhibitors. *J. Mol. Biol.* **1995**, *250*, 211–222.
- (42) Lefker B. A.; et al. 1st Winter Conference on Medicinal and Bioorganic Chemistry, 1995, Steamboat Springs, Colorado, Jan 29 to Feb 02, 1995.
- (43) Sarver, R. W.; Peevers, J.; Cody, W. L.; Ciske, F. L.; Dyer, J.; Emerson, S. D.; Hagadorn, J. C.; Holsworth, D. D.; Jalaie, M.; Kaufman, M.; Mastronardi, M.; McConnell, P.; Powell, N. A.; Quin III, J.; Van Huis, C. A.; Zhang, E.; Mochalkin, I. Binding Thermodynamics of Substituted Diaminopyrimidine Renin Inhibitors. *Anal. Biochem.* **2007**, *360*, 30–40.
- (44) Powell, N. A.; Clay, E. H.; Holsworth, D. D.; Bryant, J. W.; Ryan, M. J.; Jalaie, M.; Zhang, E.; Edmunds, J. J. Equipotent Activity in both Enantiomers of a Series of Ketopiperazine-Based Renin Inhibitors. *Bioorg. Med. Chem. Lett.* **2005**, *15*, 2371–2374 and references therein.
- (45) Tice, C. M. Renin Inhibitors. *Ann. Reports Med. Chem.* **2006**, *41*, 155–167.
- (46) Schnell, C. R.; Wood, J. M. Measurement of Blood Pressure and Heart Rate by Telemetry in Conscious, Unrestrained Marmosets. *Am. J. Physiol.* **1993**, *264*, H1509–H1516.
- (47) Ménard, J.; Boger, R. S.; Moyse, D. M.; Guyene, T. T.; Glassman, H. N.; Kleinert, H. D. Dose-Dependent Effects of the Renin Inhibitor Zankiren HCl After a Single Oral Dose in Mildly Sodium-Depleted Normotensive Subjects. *Circulation* **1995**, *91*, 330–338.
- (48) Poulsen, K.; Jorgensen, J. An Easy Radioimmunological Microassay of Renin Activity, Concentration and Substrate in Human and Animal Plasma and Tissues Based on Angiotensin I Trapping by Antibody. *J. Clin. Endocrinol. Metab.* **1974**, *39*, 816–825.
- (49) Jan Danser, A. H. Local Renin-Angiotensin Systems: The Unanswered Questions. *Int. J. Biochem. Cell Biol.* **2003**, *35*, 759–768.
- (50) (a) Cumin, F.; de Gasparo, M.; Wood, J.; Schnell, C.; Frueh, F.; Graf, P. Assays to Measure Nanomolar Levels of the Renin Inhibitor CGP 38 560 in Plasma. *Hypertension* **1989**, *14*, 379–384. (b) Wood, J. M.; Schnell, C. R.; Cumin, F.; Menard, J.; Webb, R.L. Aliskiren, a Novel, Orally Effective Renin Inhibitor, Lowers Blood Pressure in Marmosets and Spontaneously Hypertensive Rats. *J. Hypertens.* **2005**, *23*, 417–426.
- (51) Maibaum, J.; Stutz, S.; Göschke, R.; Rigollier, P.; Yamaguchi, Y.; Cumin, F.; Rahuel, J.; Baum, H.-P.; Cohen, N.-C.; Schnell, C. R.; Fuhrer, W.; Gruetter, M. G.; Schilling, W.; Wood, J. M. Structural Modification of the P2' Position of 2,7-Dialkyl-5(S)-Amino-4(S)-hydroxy-8-phenyl-octanecarboxamides: The Discovery of Aliskiren, A Potent Non-Peptide Human Renin Inhibitor Active After Once Daily Dosing in Marmosets. *J. Med. Chem.* **2007**, *50*, 4832–4844.
- (52) Yang, P.-Y.; Zhou, Y.-G. The Enantioselective Total Synthesis of Alkaloid (–)-Galipeine. *Tetrahedron: Asymmetry* **2004**, *15*, 1145–1149.
- (53) Hackenthal, E.; Hackenthal, R.; Hofbauer, K. G. No Evidence for Product Inhibition of the Renin-Angiotensinogen Reaction in the Rat. *Circ. Res.* **1977**, *41*, 49–54.